The Relativity Mission Gravity Probe B, Testing Einstein's Universe

SAPS BUCHMAN for the GP-B COLLABORATION

Stanford University, Hanson Experimental Physics Laboratory, Stanford, CA 94305, USA

The Relativity Mission, Gravity Probe B (GP-B) is the most complex gravitational space experiment to date and the first controlled experiment in which a General Relativistic effect is the main feature of the data. Launched on April 20, 2004 it has successfully taken science data from August 29, 2004 to August 15, 2005. Using four high precision gyroscopes GP-B measures the relativistic precessions of the frame of reference in a 642 km polar orbit. The two precessions are predicted in General Relativity to be the geodetic effect, 6.6 arcsec/year, and the frame dragging effect, 0.042 arcsec/year. Comprehensive pre and post mission calibrations have been performed between April 20 and August 27, 2004 and between August 15 and September 29, 2005. GP-B is the first experiment to see General Relativity directly as the main effect of the measurement and has demonstrated that very complex physics experiments can perform flawlessly in space. We present engineering performance data and general operational information for the major systems of the mission. Lessons learned from the GP-B experience and their impact on the development of technology for the Laser Interferometer Space Antenna (LISA) and the Space Test of the Equivalence Principle (STEP) are discussed. Technology progress for the design of the next generation of drag-free sensors is presented. Preliminary results set the measurement accuracy at ± 97 marcs/year or about ± 1.5% of the geodetic effect. The GP-B science team is continuing to refine the analysis of the data and further improvements in accuracy are expected. Final science results will be released in December 2007.

Introduction

At a banquet honoring Albert Einstein in 1930 George Bernard Shaw aptly summarized the quest for understanding the Universe in the last two thousand years:

"...there is an order of men who are makers of Universes. Ptolemy made a Universe which lasted fourteen hundred years. Newton also made a Universe which has lasted three hundred years. Einstein has made a Universe and I can't tell you how long that would last."

This progression exemplifies beautifully the approach to the truth through consecutive approximations. Ptolemy's empirical model used eighty epicycles to explain the motions of the Sun, the Moon, and the five known planets. It matched visual observation to their level of accuracy and was "the Universe" for thirteen centuries. Copernicus's heliocentric system (1543) and Keppler's three laws (1618) were the start of the modern description of planetary motion. Newton's Universe, based on the equivalence of the inertial and the gravitational mass is in many ways the beginning of modern science. The limit on the equivalence principle is presently about 10^{-13}.

In 1915 Einstein formulated General Relativity based on the equivalence of gravitational and acceleration fields, describing gravity as the curvature of space, and establishing the equality between the space-time Einstein tensor $G_{\mu\nu}$ and stress-energy tensor $T_{\mu\nu}$ (equation 1)

$$G_{\mu\nu} = \frac{8\pi G}{c^4} T_{\mu\nu} \qquad G_{\mu\nu} \equiv R_{\mu\nu} - \frac{1}{2} R g_{\mu\nu} + \Lambda g_{\mu\nu} \tag{1}$$

where $R_{\mu\nu}$ is the Ricci tensor, R the Ricci scalar, and $g_{\mu\nu}$ the metric tensor, and Λ Einstein's cosmological constant.

General Relativity remains the longest lived modern physical theory. Early on it has resolved the 43 arcs/century discrepancy in the perihelion shift of Mercury, it has correctly predicted the deflection of light by the Sun (1.75 arcs during the 1919 eclipse) and the redshift in a

gravitational field. Its predictions, including the once believed implausible black holes, have all been confirmed by measurements and observations. General Relativity remains an elegant and the most widely accepted theory of gravitation, that agrees with experimental results to better than 10^{-4}. In the fast moving modern science of the last century General Relativity has lasted amazingly long and has been spectacularly successful.

Why then test Einstein? The main question remains the problem of unified physics. General Relativity is not quantizable and thus incompatible with the Grand Unification theories that unite the electromagnetic, strong nuclear, and weak nuclear forces. Grand Unification theories predict violations of General Relativity and the promising areas to discover discrepancies are in rotational effects, below the 10^{-5} level, and in the equivalence principle, below the 10^{-14} level.

Section 1 discusses the rational for performing gravitational experiments in space, and describes the GP-B mission. Section 2 summarizes the performance of the main GP-B systems and the results to date. The LISA and STEP mission concepts and their common technologies with GP-B are summarized in section 3. Section 4 discusses the lessons learned from GP-B and their applications to LISA and STEP. Section 5 describes advances in the area of drag-free technology with applications to future gravitational space missions.

1 The GP-B Experiment

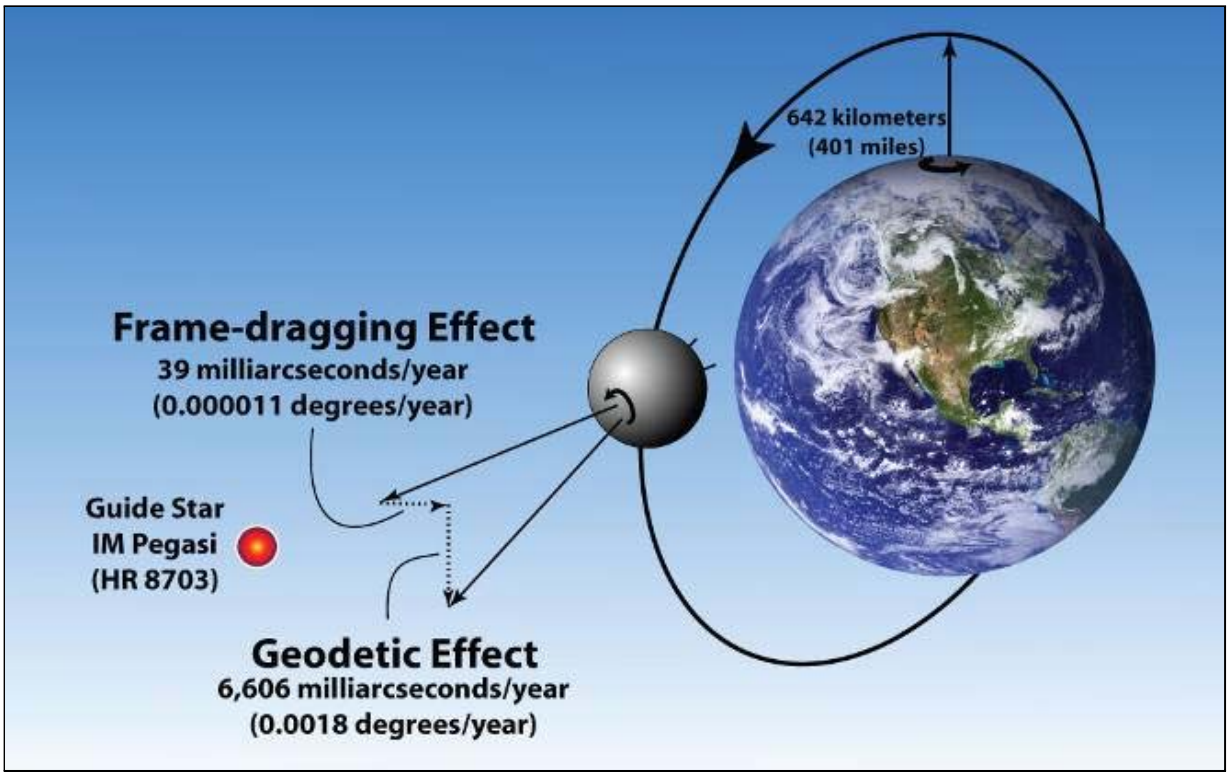

Figure 1: The Relativity Mission, Gravity Probe B concept.

"No mission could be simpler than Gravity Probe B. It's just a star, a telescope, and a spinning sphere." – William Fairbank

GP-B is measuring two rotational effects predicted by gravitational theories; the geodetic precession due to the distortion of space by a massive body, and the frame dragging precession, a twisting of space caused by the rotation of the body.[1] [2] Earth is the massive body, with the experiment in a 642 km polar orbit. Figure 1 shows this very simple concept of GP-B. The frame

of reference in the field of the Earth, measured by gyroscopes, is compared to the reference frame of distant stars determined by a telescope locked on a guide star. The guide star is HR8703 (IM Pegasi) a binary with optical and radio frequency emissions. Its proper motion with respect to Quasars is determined by VLBI measurements. Equation 2 gives the two precessions as computed in General Relativity and expanded in the Parameterized Post Newtonian (PPN) formalism used for metric theories in weak gravitational fields. The geodetic precession in the plane of the polar orbit, first term, and the frame dragging orthogonal to the orbit plane, second term, are proportional respectively to the mass and the moment of inertia of the Earth.

$$\overline{\Omega} = \left(\gamma + \frac{1}{2}\right) \frac{GM}{c^2 R^3} \left(\overline{R} \times \overline{v}\right) + \left(\gamma + 1 + \frac{\alpha_1}{4}\right) \frac{GI}{2c^2 R^3} \left[\frac{3\overline{R}}{R^2} \cdot \left(\overline{\omega}_e \cdot \overline{R}\right) - \overline{\omega}_e\right]. \qquad (2)$$

GP-B is a unique gravitational measurement in space, as a controlled physics experiment with an apparatus specifically designed for the purpose with fully determined parameters. While based on a simple concept, the precision requirements make GP-B a very complex experiment based on cutting edge technology, never before used in space. Its superb performance demonstrates that such complex experiments can and will work and greatly increases the confidence in the success of future experiments in space.

Figure 2 shows the preliminary analysis results of the direct measurement of the geodetic effect, the north-south inertial orientation of the four gyroscopes to ±1.5% (±97marcsec/yr).

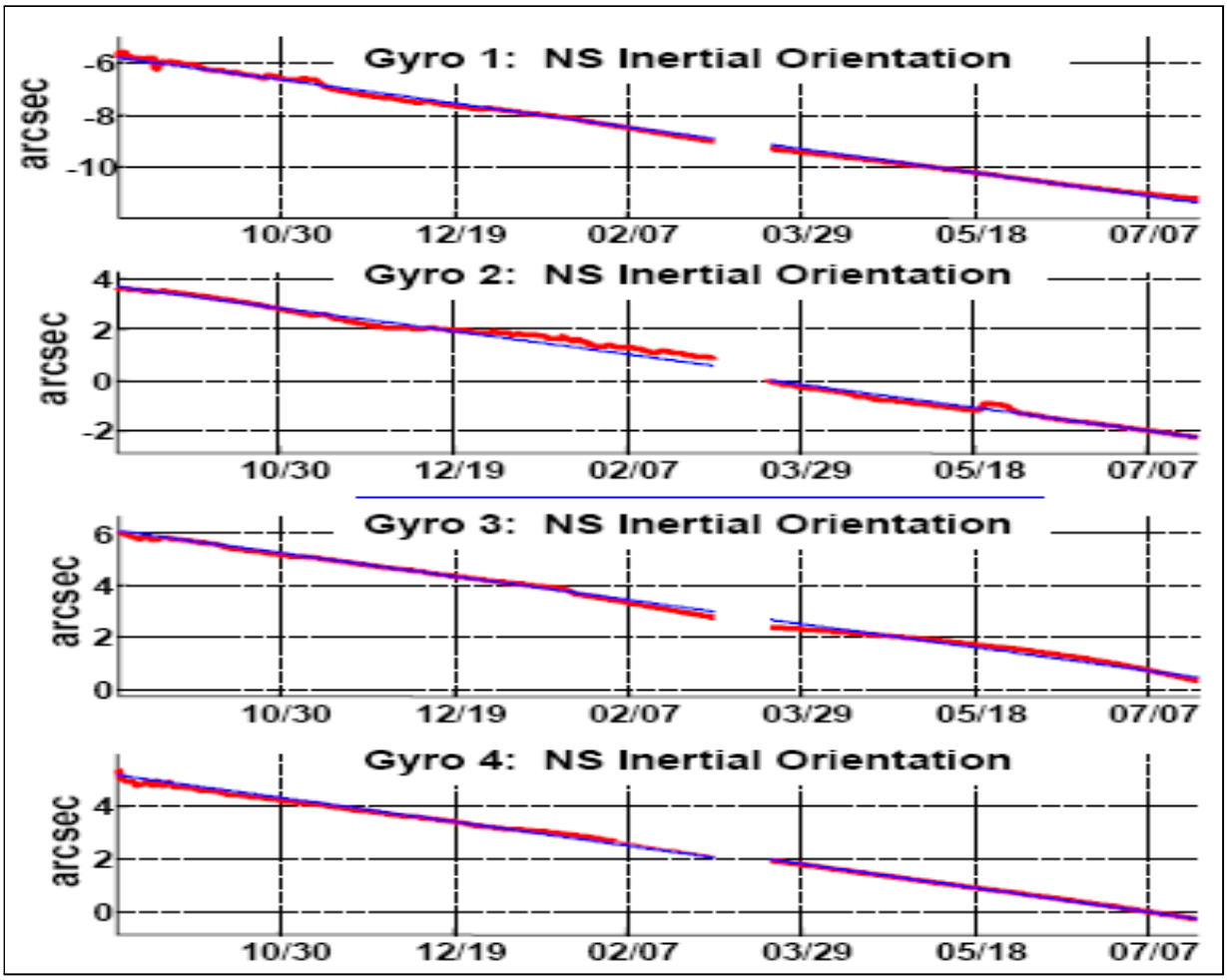

Figure 2: Geodetic effect seen directly; raw data in red, with torque analysis, blue.

Present measurement limitations (April 2007) are mainly due to incomplete torque modeling,

interuptions in the data stream, roll phase uncertainties, and systematic read-out errors. The SQUID readout noise is contributing less than 1marcs/yr to the error. Note: deg/hr are the units habitually used for gyroscope drift: 1 marcs/yr = 3.2×10^{-11} deg/hr. Fragmentation of the year-long data stream, caused by annomalies, torques, and data analysis approaches, will reduce the nominal measurement accuracy $\delta\Omega$ to $\delta\Omega_n$ proportionally to the number n of segments (considered equal for this example); equation 3.

$$\delta\Omega = L \cdot T^{-3/2} \qquad \delta\Omega_n = L \cdot T^{-1/2} \cdot t^{-1} = \delta\Omega \cdot n \tag{3}$$

where L is the proportionality constant, T is the nominal science duration, t the segment length and $n \equiv T/t$.

The spacecraft rolls phase locked around the line of sight to the guide star (telescope axis) with a period of 77.5 seconds. This results in the spectral shifting of the science signal from zero frequency to 12.9 mHz (the gyroscope 1/f read-out noise is reduced) as well as in the averaging of the body fixed disturbance torques acting on the gyroscopes. The averaging is proportional to the angle of about 20 arcs between the telescope axis and the spin axes of the gyroscopes, equivalent to a reduction in disturbance by 10^4. The roll phase is determined by star trackers and used to separate Einstein's predicted gyroscope spin-axis drifts.

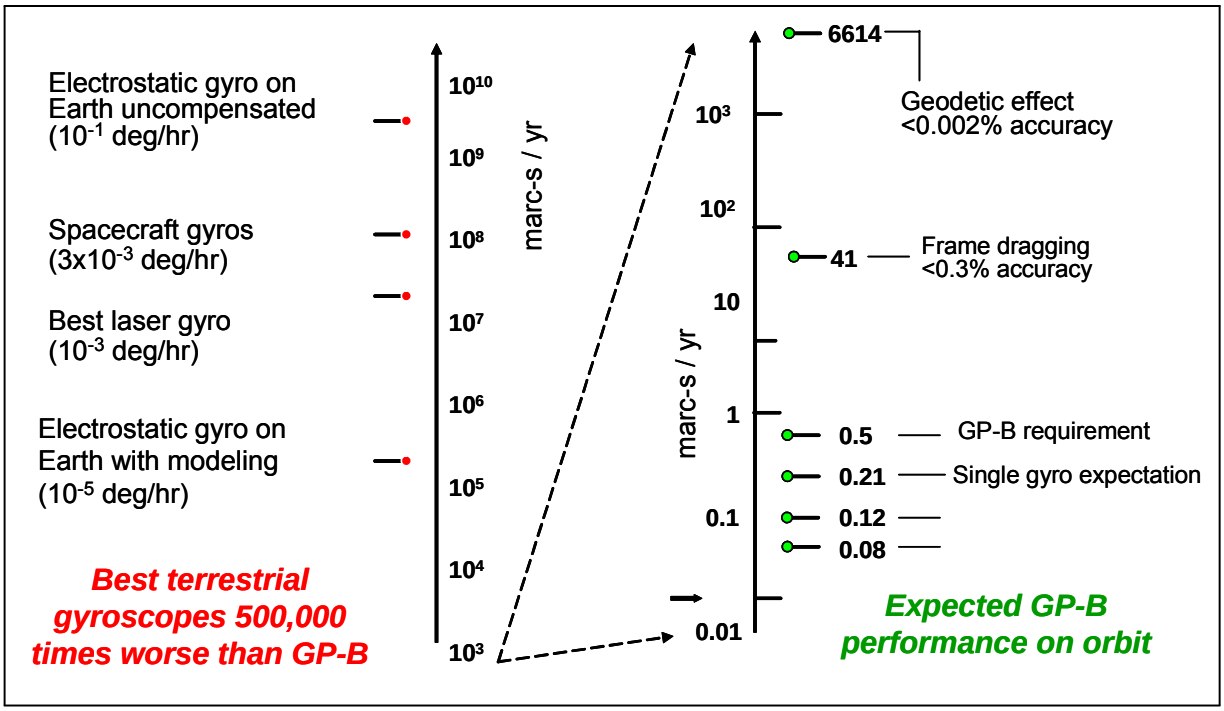

Figure 3: GP-B gyroscopes in space versus ground based gyroscopes.

Deciding on performing a space experiment requires the careful balancing of the advantages and disadvantages of space. Such experiments are costly and of very long duration, require survivability in the severe launch environment, are a single opportunity endeavor with any major anomaly potentially causing total mission loss, and are handicapped by limitations in communications. However, low seismic noise in the frequency region below 1 Hz, the low gravity environment, long interferometry baselines, and long integration times make space the only possible way of achieving the requirements for a number of experiments including GP-B, LISA, and STEP. Table 1 summarizes the main advantages and disadvantages of space experimentation, while figure 3 shows the rational behind performing GP-B in orbit. Only the very low gravity

of space allows the gyroscope performance required for the measurement of the relativistic precessions. GP-B is the first experiment to directly measure gravitational relativity as the main measured effect.

Table 1: Main advantages and disadvantages of space experiments.

Experimentation in space	
Advantages	**Disadvantages**
Low seismic noise below 1 Hz (LISA)	High acceleration launch
Low acceleration; $< 10^{-10}$ m/s^2;GP-B,LISA,STEP	High cost and long development
Long baselines; 5×10^6 km for LISA	Single opportunity: high reliability req.
Long measurement times (GP-B, LISA, STEP)	Restricted communications band

2 GP-B Performance

GP-B was launched on April 20, 2004. The Delta II rocket placed the space vehicle in within 100 m of the required orbit. Figure 4 shows the nearly perfect insertion point in relation of the "target lens" the required final orbit area. The quality of the insertion made orbit adjustment unnecessary and therefore allowed for simplified experiment initialization.

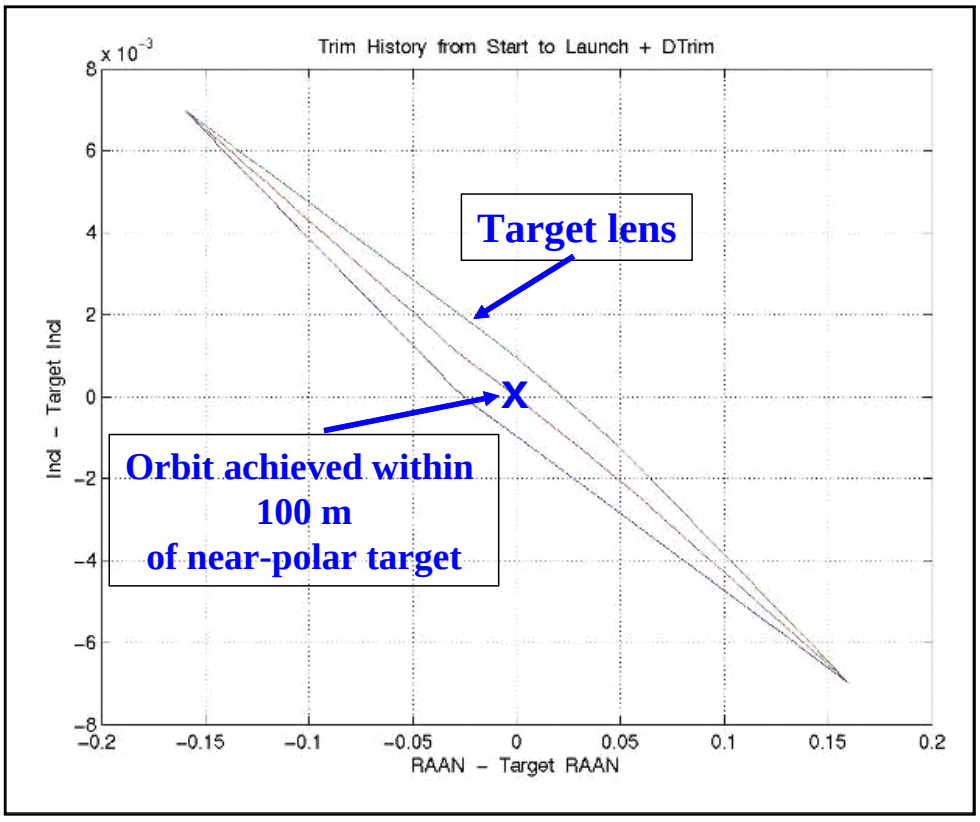

Figure 4: GP-B orbit insertion

Until Science Mission start, on August 29, 2004, the experiment underwent a period of 128 days of initialization that included instrument calibrations, guide-star acquisition, spacecraft

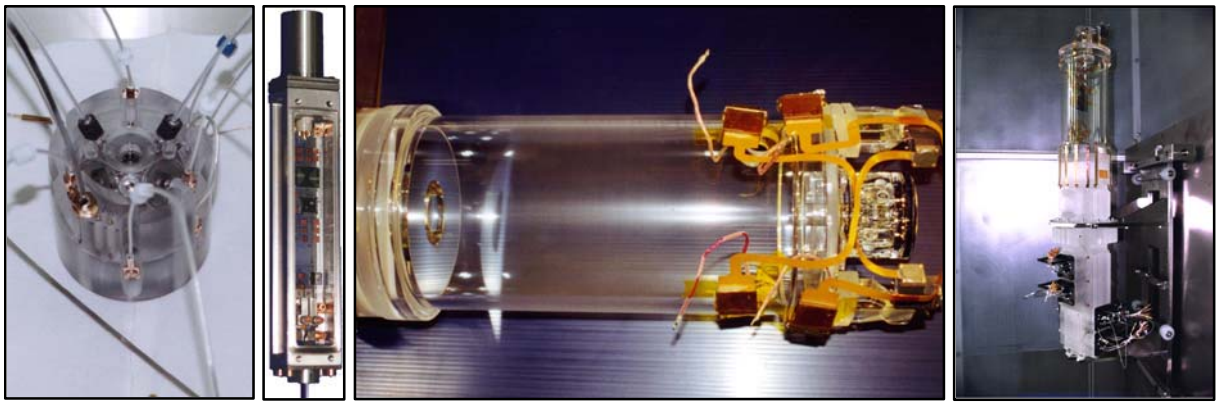

Figure 5: Assembled gyroscope, dc SQUID, telescope, and SIA

Table 2: GP-B critical “near-zeros" and superlatives: requirements and performance in orbit.

#	Systems	Requirement	In orbit performance
1	Rotor asphericity	< 50 nm	< 10 nm
2	Rotor inhomogeneity	< 25 nm	< 7nm
3	Electric charge	< 15 pC	<15 pC
4	Residual acceleration	$< 10^{-12}$ m/s^2 at roll	$< 10^{-12}$ m/s^2 at roll
5	Gas pressure	$< 10^{-11}$ torr	$< 10^{-14}$ torr
6	Magnetic field	< 9 μG in rotor	< 3 μG in rotor
7	Low-noise SQUID	< 200marcs/$\sqrt{\text{Hz}}$at roll	< 190marcs/$\sqrt{\text{Hz}}$atroll
8	Sensitive star-tracker	0.1 marcs	0.1 marcs
9	Largest flight dewar	2,500 l, 16.5 month, 1.8K	2,500 l, 17.3 month, 1.8K
10	Star proper motion	< 0.3 marcs/year	< 0.15 marcs/year

rolling, drag-free set-up, spin-up of gyroscopes and their alignment with the roll axis, and low-temperature bake-out. The 128 days was triple the expected duration of 40 days and more than twice the 60 days initialization allocation with contingency margin, notwithstanding the excellent communication bandwidth provided by the ground and space NASA networks. Thus, the first GP-B lesson learned is to allow for a factor of three contingency in the planned experiment initialization period. The science data collection phase lasted for 353 days until August 15, 2005. In addition to the collection of science data, redundancy and internal cross-checks of these data were performed. The 46 day calibration phase, ending with the depletion of the liquid helium on September 29, 2005, consisted of repeat calibrations while deliberately enhancing the disturbing effects.

The GP-B, Science Instrument Assembly (SIA), contains four electrostatically suspended cryogenic gyroscopes, four dc SQUID read-outs, and a14 cm aperture 380 cm focal length Cassegranian telescope, all mounted in a quartz block that ensures accurate and stable alignment; figure 5. Each gyroscope is sufficient for the GP-B experiment, thus the local frame is measured with quadruple redundancy while the telescope has double redundancy for measuring the far-stars reference frame.

The SIA is mounted in the cryogenic probe, that is in turn inserted in the dewar. The spacecraft systems are mounted around the dewar that supplies the mechanical core of the space vehicle; figure 6.

We present the GP-B instrumental performance in terms of the cutting edge technologies for the mission that were never before achieved in space or, in some cases, even on the ground.

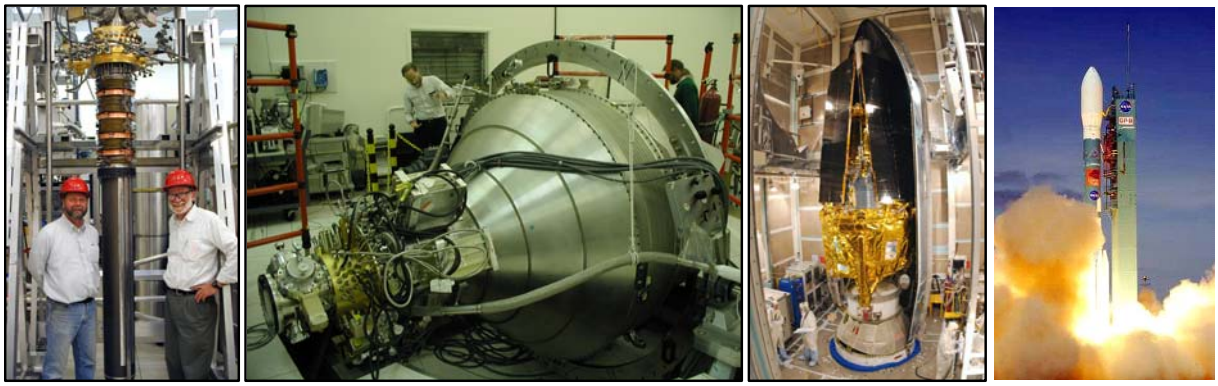

Figure 6: Cryogenic probe, dewar, space vehicle in faring, GP-B launch April 20, 2004.

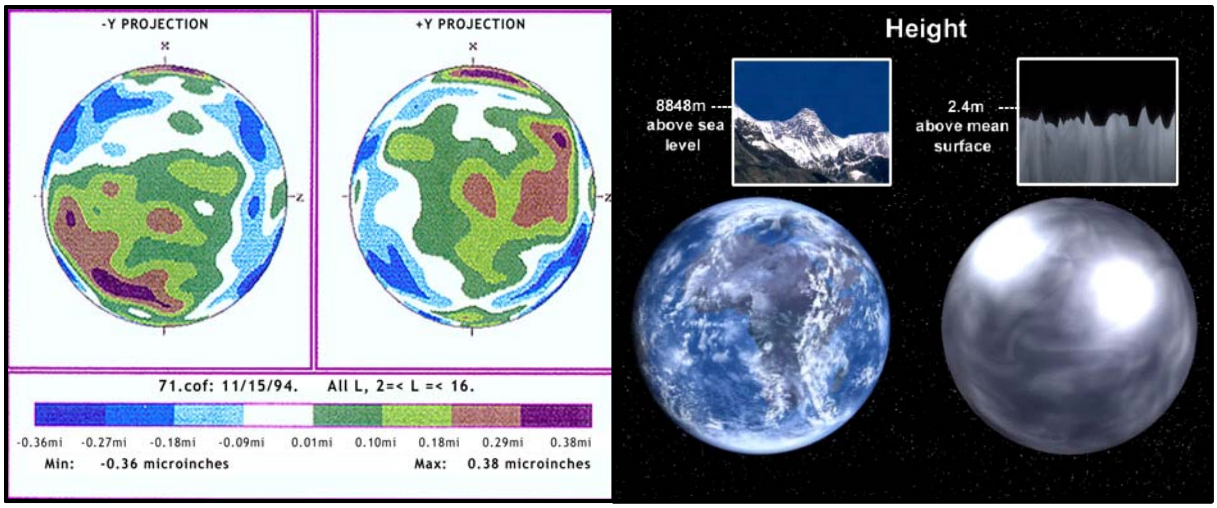

Figure 7: Surface profile of GP-B flight rotor (spherical to 0.2 ppm) and its equivalent scaling to Earth size.

Table 2 lists the ten "Near-zeroes and Superlatives", their performance requirements and their actual measured performance in orbit. All requirements were achieved or surpassed.

The gyroscopes are at the core of the GP-B mission. The reference to the universal frame, the telescope, is required to perform 10^3 times better than the best prior star trackers, while the reference to the local frame, the gyroscopes, are required to have drifts up to 10^7 times smaller than the best modeled previous instruments. Most of the ten "near-zeroes" and superlatives are therefore technologies required to achieve the gyroscope performance. The main features of the GP-B gyroscopes are: electrical suspension and position measurement, Helium gas spin-up, magnetic read-out, and cryogenic operation. Sphericity uniformity is critical to the performance of the gyroscopes by minimizing the torques caused by the electrostatic fields. The gyroscopes are 3.9 cm diameter fused quartz spheres coated with 1μm thick Niobium film of 2% uniformity. Quartz substrate sphericity is $2 \cdot 10^{-7}$ of diameter or less than 10 nm peak-to-valley; gyroscope housing uniformity is about one magnitude less. Figure 7 shows the color coded surface profile of a flight rotor mapped to 1 nm precision and its equivalent surface roughness if expanded to the size of the Earth.The centered gyroscopes are spaced at 32 μm from the suspension electrodes with a maximum clearance of 20 μm from other housing features. In order to reduce precession the center of mass coincides to the center of geometry (mass unbalance) to $2 \cdot 10^{-7}$ of diameter. Figure 8 shows the measurement method of the mass unbalance using the maximum of the range

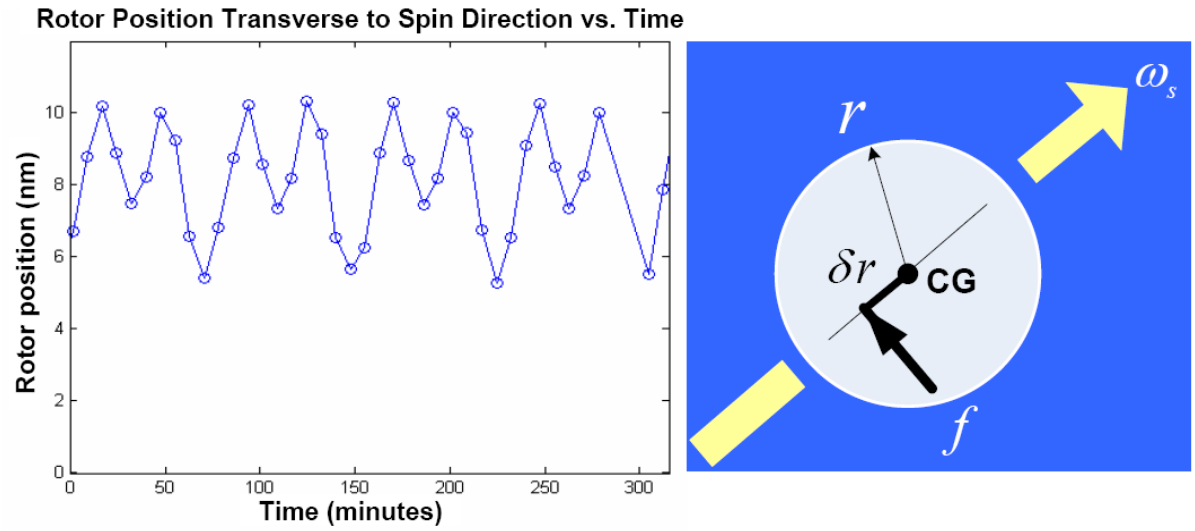

Figure 8: Gyroscope mass unbalance δr measured by maximum variation of position transverse to spin direction.

Table 3: Mass unbalance: pre-launch estimate and on-orbit data.

Gyro #	Pre-launch estimate (nm)	On-orbit data (nm)
1	18.8	10.1
2	14.5	4.8
3	16.8	5.4
4	13.5	8.2

of positions of the gyroscope as swept by its polhoding motion; on the right is the schematic of the forces moving the mass unbalance δr with respect to the spin axis. Table 3 shows the pre-launch estimates of the mass unbalance versus the measurements on orbit. The mass unbalance values are well below the requirement of 50 nm.

Table 4: Spin speed and spin-down rates.

Gyro #	Spin-speed (Hz)	Spin-down rate (μHz/hour)
1	79.4	0.57
2	61.8	0.52
3	82.1	1.30
4	64.8	0.28

The GP-B gyroscopes were spun up in orbit with Helium gas warmed to 6.5 K, below the superconducting transition of their Niobium coating. Spin-up proceeded by bringing the gyroscopes close to the channel through which Helium flows at 750 cm^3/min. 95% of the gas is being exhausted directly to space through dedicated pumping lines, while the remaining 5% are pumped through the instrument. The leakage gas limits the flow rate of gas for spin-up and causes some slow-down of the other gyroscopes. Figure 9 shows the first gyroscope suspension and the spin-up of gyroscope #1. Gyroscope #1 was spun-up last; its spin-up causes some spin down of the other gyroscopes. Table 4 gives the science mission spin-speed and average spin-down rate for each of the four gyroscopes.

The gyroscope charge was controlled to less than 15 pC; equivalent to a potential of 15 mV

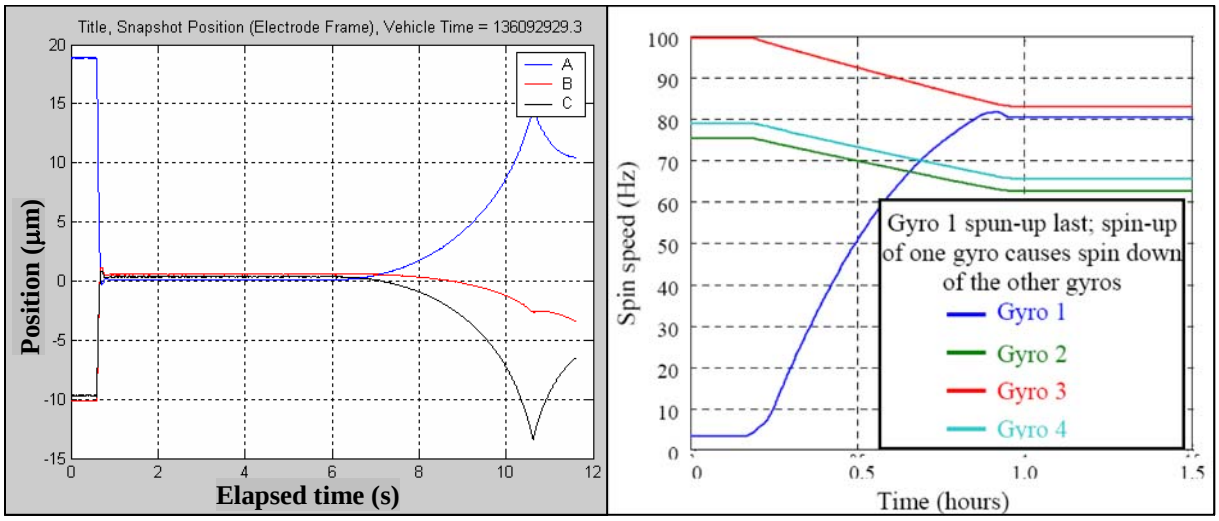

Figure 9: First gyroscope suspension and GP-B gyroscope spin-up.

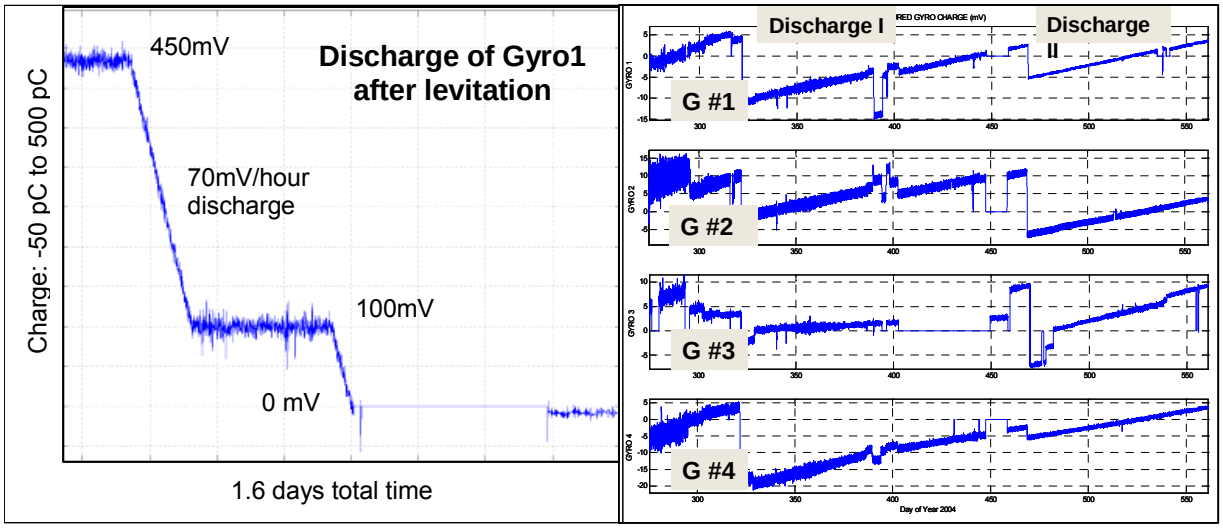

Figure 10: a) Discharge of Gyro 1 after levitation. b) Charging and discharging of the GP-B gyroscopes; 5 mV/div vertical, 50 days/div horizontal.

for the 1 nC total gyroscope capacitance. Charge management was achieved by UV generated photoelectrons from the gyroscope and housing, which were moved onto or away from the gyroscope by the appropriate electrostatic bias.[5] The charge was measured to better than 2 pC by applying out of phase 20 mV potentials to opposite electrodes at about 50 mHz.

As expected, two main charging mechanisms required management. The largest by far, was the one time charge of between 200 pC and 500 pC generated by the separation of dissimilar metals during initial gyroscope levitation. In order to achieve science electrostatic suspension mode this charge needed to be reduced to less than 15 pC; figure 9. During science mission the charging was caused by cosmic radiation at a daily rate of 0.1 pC to 0.15 pC. During a major solar flare (sun spot 720) the charging rates increased to between 0.6 pC/day and 1.2 pC/day. As calculated prior to launch, the cosmic radiation charging was always positive and caused mainly by protons stopping in the gyroscope. In order to maintain the charge below 15 pC only two discharge operations were required during the mission, at 3 months and 7 months after science start. Figure 10a shows the discharging of gyroscope #1 after levitation. The

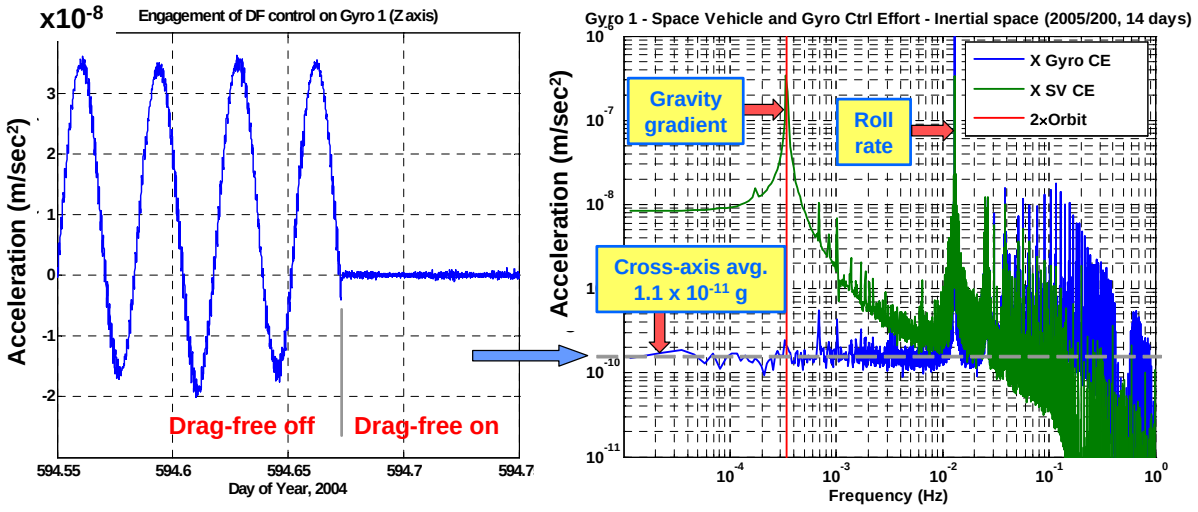

Figure 11: Acceleration of drag-free gyro: drag free off and on

initial charge from levitation was 450 pC and the discharge rate was 70 pC/hour. Figure 10b shows the charge history of the four gyroscopes, including the two discharge operations; scale is 5 mV/division vertical and 50 days/division horizontal.

Gyroscope performance is dependent on the level of drag-free the control systems are reaching.[6] By controlling the position of the spacecraft around a test mass, in the case of GP-B a gyroscope, drag-free technology reduces the disturbing acceleration effects in orbit as caused principally by radiation pressure and residual gas. The average acceleration transverse to roll axis was approximately 10^{-10} m/s^2. Figure 11 shows the acceleration level with drag-free off, left, and drag free on, right.

Cutting edge technology, which can only be tested by analysis and simulation on the ground, requires maximum flexibility in the modes of operations, incorporating as many software 'hooks' as practical. An example is provided by the three modes of operation of the electrostatic suspension of the GP-B gyroscopes. In the accelerometer mode the position of the gyroscope is the input for the control provided by the electrostatic suspension. This mode is used for science in three of the four gyroscopes as well as for levitation, calibrations, spin-up, and spin alignment. The drag-free mode uses the gyroscope position measurements as input for the control system of the space vehicle thrusters while the gyroscope electrostatic suspension is turned off. This is a possible science mission mode for the drag-free sensor gyroscope. For flexibility, GP-B has also provided a third mode, the back-up drag-free. It uses the space vehicle thrusters as primary actuators to minimize the gyroscope suspension control effort and the electrostatic suspension for fine tuning of the gyroscope position. The performance of the back-up drag free system has been shown in orbit to be better and more reliable then the primary drag-free, and was therefore used during the entire science mission. Figure 12 shows the three suspension modes; the three axes in the space vehicle coordinates for the position and control effort of gyroscope #3 and the space vehicle forcing.

GP-B's attitude and control (ATC) and drag-free systems pose a 9 degrees of freedom (DOF) problem with complex dynamics and coupling. The integrated system actively controls 9 interacting DOF: 3 in attitude of spacecraft to track guide star and maintain roll phase (using thrusters), 3 in translation: drag-free about the geometric center of the gyroscope housing (using thrusters), and 3 in translation of the gyroscope with respect to its housing (using the gyroscope suspension system); figure 13. Figure 14 shows the three main mechanisms used by the space vehicle for ATC and drag-free control; from left to right (not to scale) a proportional Helium

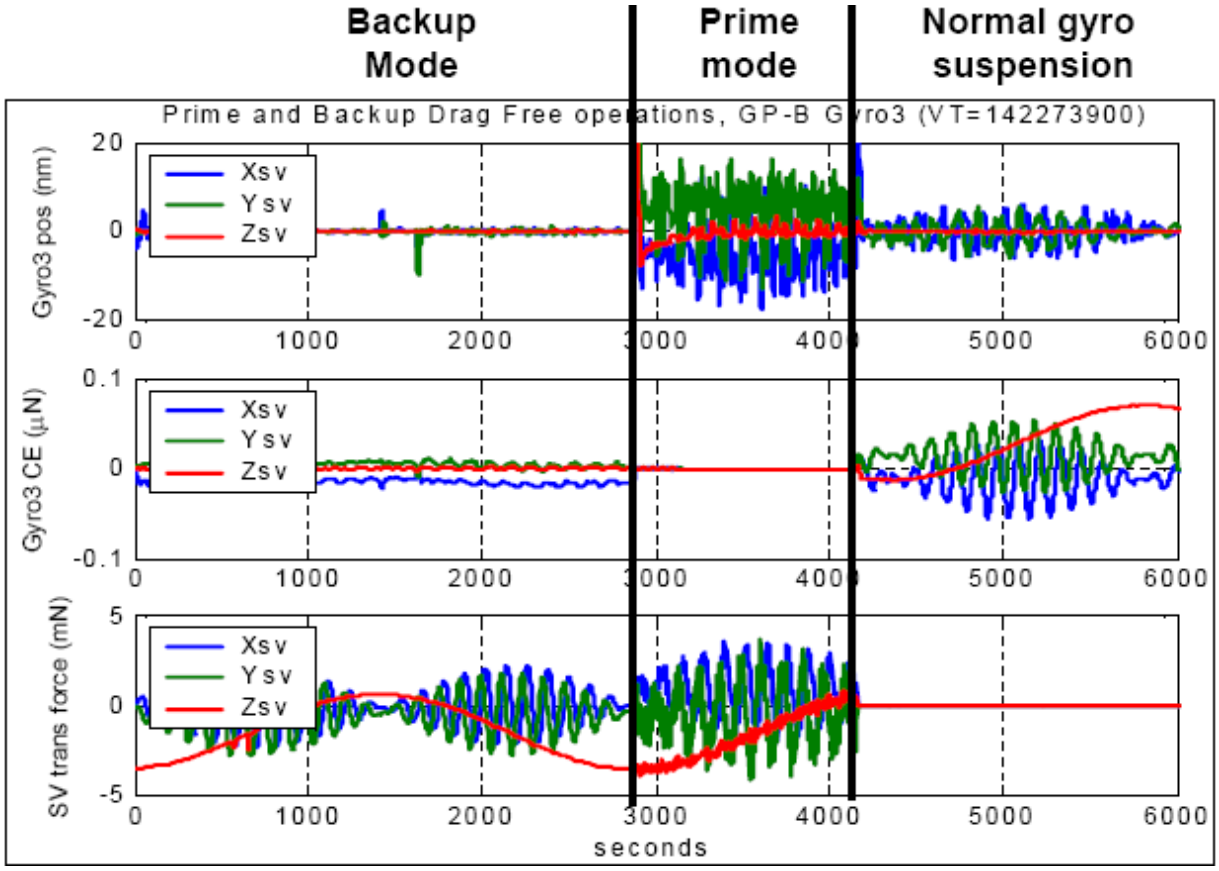

Figure 12: The three suspension modes of the GP-B gyroscopes.

thruster cut-out, a star tracker, and a mass trim mechanism used to adjust the center of mass and the axes of inertia of the space vehicle. Including the redundant systems, the GP-B space vehicle has a total of 16 thrusters 2 star trackers, and 7 mass trim mechanisms. Orbital position and velocity were determined by a GPS system, a commercial system modified by Stanford. The modifications included hardware upgrades for space use and sophisticated new software that allowed the system to track the GPS constellation while the space vehicle was both orbiting Earth and rolling with a 77.5 period around its axis. The GPS was the main data source for orbit determination, with a secondary back-up of laser ranging from corner cubes. One of the two fully redundant sets of receivers with four antennas each provided position, velocity, and time data every 10 seconds; more than 5000 points per day. The GP-B rms position and velocity accuracy requirements were 25 m and 7.5 cm/s. The actual achieved accuracies were 2.5 m rms and 2.2 mm/s rms; 10 and 35 times better than required.

Table 5 gives the details of the control systems used for GP-B, the first precission controlled six degrees of freedom spacecraft. Abbreviations: DOF=degrees of freedom, GS=guide star, ST=science telescope, STr=star tracker, MT=micro thruster, SC=spacecraft, I=moment of inertia of spacecraft, CM=center of mass of spaceccraft, MTM=mass trim mechanism.

Since the gyroscopes are not at the center of mass of the space vehicle, the small differences in gravity due to the differences in the distance to Earth, the gravity gradients, can be seen as forces on the gyroscope of about 10^{-6} m/s^2. Figure 15 shows the increased control effort of the suspension system due to the gravity gradient while the gyroscopes operate as accelerometers. The demonstrated accelerometer performance is better than 10^{-12} m/s^2 from 0 Hz to 1 Hz. The gravity gradient varies at twice orbital frequency.

The gyroscopes are spun with Helium gas in orbit. To remove the remaining Helium, the

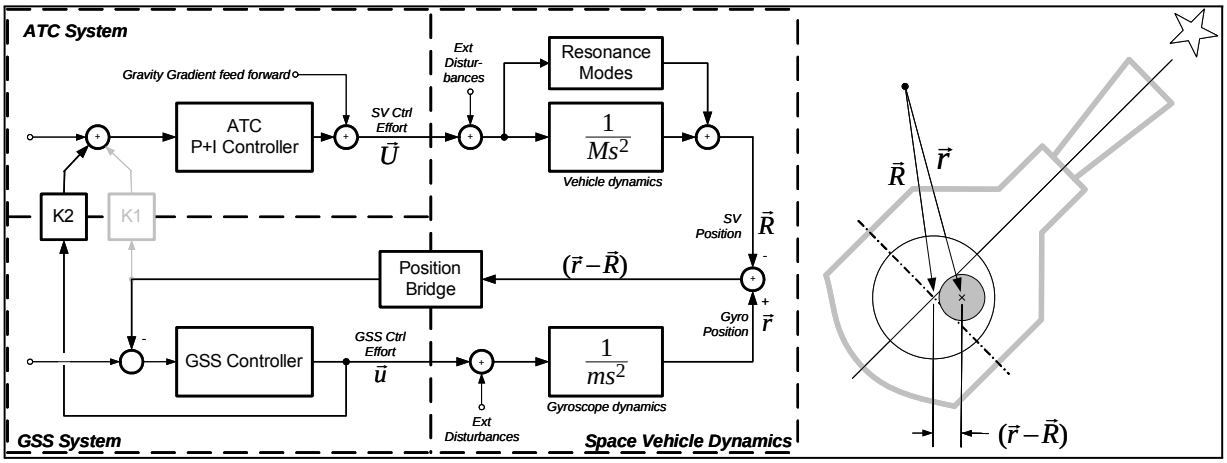

Figure 13: Schematic of the GP-B 9 DOF drag-free and ATC control systems.

Table 5: Six degrees of freedom spacecraft control.

Controller	DOF	Requirement	Sensor	Actuator	Control computation
GS pointing	2	20 marcs	ST	MT	SC computer
Drag-free	3	10^{-12}m/s^2 rms	GSS	MT	SC computer
Other gyros		0.3nm at 13mHz	GSS	GSS	GSS
SC roll	1	20 arcs rms	STr	MT	SC computer
Orbit		<500m from Pole	GPS	MT	SC computer
SC max I		MT capability	MT demand	MTM	On ground
SC CM		0.3 mm	GSS	MTM	On ground

entire apparatus is heated to 6 K, evacuated to space, ($5{\cdot}10^{-9}$ torr to 10^{-8} torr), isolated from the environment by closing all exhaust valves, and finally cooled down to the approximately 1.8 K science working temperature. The pressure in the apparatus at 1.8 K, as determined from experiments at higher temperatures is about 10^{-14} torr. Table 6 gives the average spin-down periods before and after bake-out. Figure 16 shows the spin-down rates and implied pressures before, during, and after the bake-out. The spin-down rates after bake-out are not dominated by gas differential damping.

GP-B's magnetic readout requires both ultra-low magnetic field at the instrument location and very high magnetic shielding of outside sources. Taking advantage of the conservation of magnetic flux in a superconducting loop, magnetic fields of less than 10^{-7} gauss are achieved by

Figure 14: Helium thruster, star tracker, mass trim mechanism (not to scale).

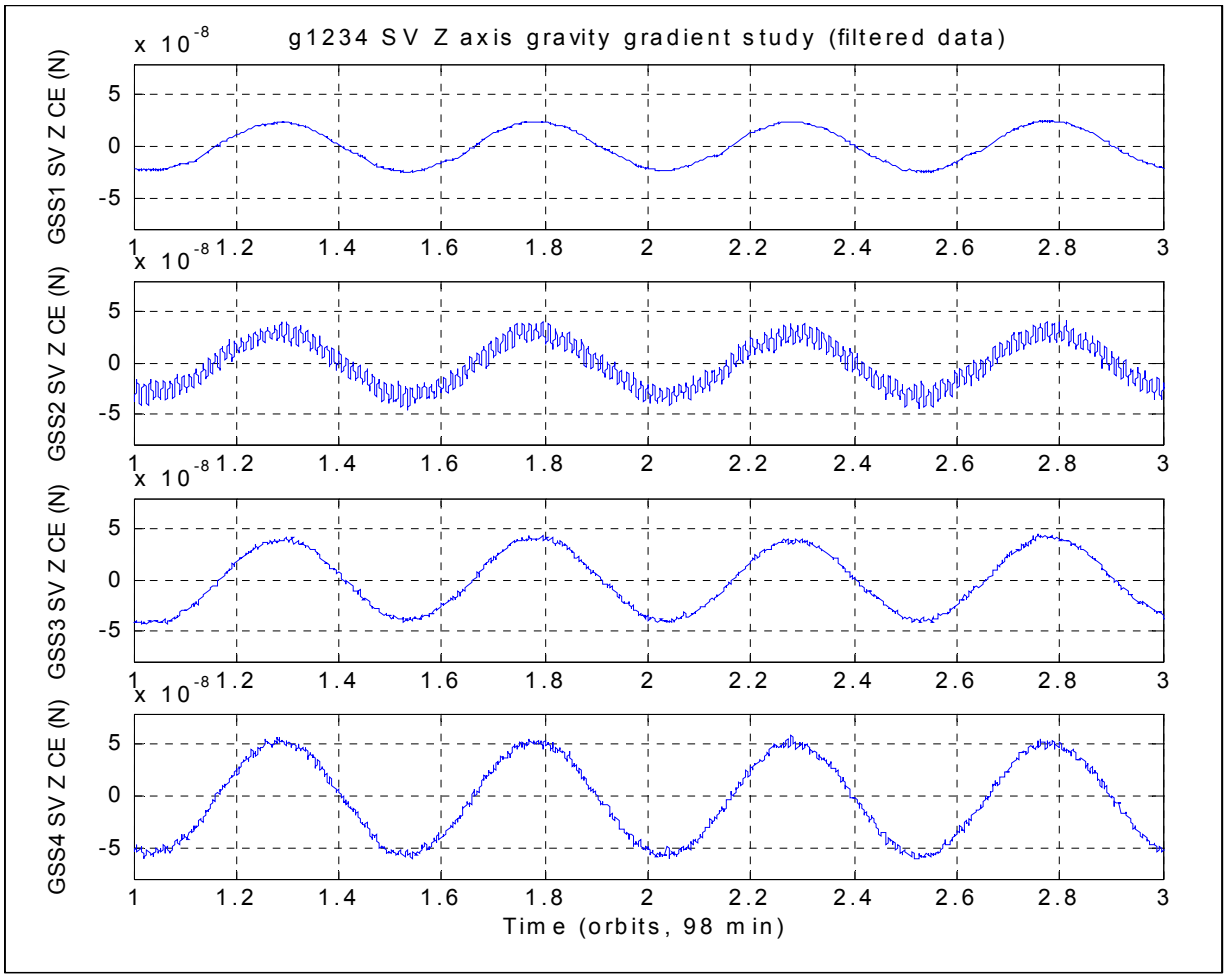

Figure 15: Gravity gradient for the gyroscopes in accelerometer mode.

the expansion of a series of nested lead bags.[7] A system of magnetic shields, including the lead bag, attenuates the external field by 120 db. Table 7 gives the trapped field in the gyroscopes superconducting coating as measured in orbit. Note that the trapped field decreases with the depth of the gyroscope location inside the lead bag.

The spinning superconducting gyroscopes develop magnetic dipoles, also called the London moment, aligned with the spin axis and, for the uniform spherical gyroscopes, with the angular momentum. Figure 17 shows the schematic configuration of the GP-B read-out, based on the coupling of the London moment flux through a superconducting read-out coil to a dc SQUID. Equation 4 gives magnetic field in gauss as a function of the angular spin frequency ω and the electron mass and charge. The readout sensitivity is 190 marcs/$\sqrt{\text{Hz}}$ (5×10^{-11} G/$\sqrt{\text{Hz}}$) at 12.9 mHz roll frequency, figure 18. Table 8 gives the SQUID noise in $\mu\Phi_0/\sqrt{\text{Hz}}$ and in marcs/$\sqrt{\text{Hz}}$ as well as the read-out limit for a year of integration. Figure 19 shows the SQUID output data for the guide star valid portion of the orbit; the roll frequency output is modulated by the orbital aberration.

$$\overline{B}_L = -\frac{2m_e c}{e}\overline{\omega}_s = -1.14\cdot10^{-7}\overline{\omega}_s \text{ (gauss)} \tag{4}$$

The GP-B telescope, used as a very high quality star tracker, has a folded Cassegranian configuration. For instrument geometry optimization a tertiary mirror returns the image to the

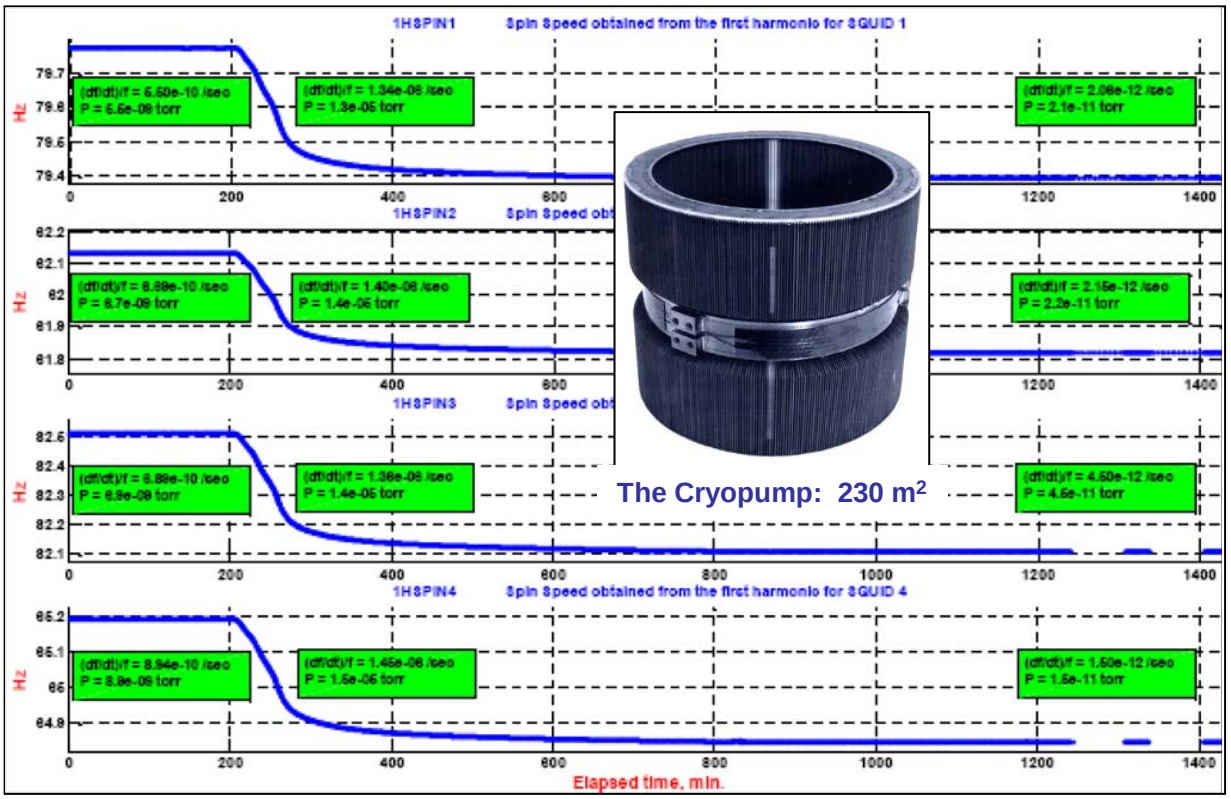

Figure 16: Spin-down rates and presures before, during, and after bake-out. Insert cryopump picture.

Table 6: Spin-down periods (years) before and after bake-out.

Spin-down periods on orbit (years)		
Gyro #	Before bake-out	After bake-out
1	75	15,900
2	62	13,600
3	60	7,200
4	46	26,400

front end. Image dividers split the beam in orthogonal components with double redundancy read-out. The sensors are silicon detectors working at 72 K; with two sensors per detector assembly, figure 20. The telescope points to the guide star (GS) during about half the orbit, GS valid, and is obscured by the Earth during the other half, GS invalid. Figure 22a shows the telescope pointing data during GS valid. The star is acquired in less than 1one minute; September 9, 2004, 54 minutes total science data. The telescope measurement precision is 0.1 marcs, with its pointing of 34.5 marcs/$\sqrt{\text{Hz}}$ determined by the Helium thruster noise.

Calibration and matching of the scale factors of the telescope and gyroscope is done by two methods. Firstly a slow (29 s and 34 s for the x and y axes) of 60 marcs amplitude was applied with the ATC system allowing scale factor matching for accurate subtraction. Secondly the orbital and annual aberration of the guide star was used to provide the absolute calibration of gyroscope read-out. The motion of the Earth around the Sun causes an annual aberration of 20.4958 arcs, while the motion of the space vehicle around the earth causes an orbital aberration of 5.1856 arcs (at the 97.5 min. orbital period). Figure 21 shows the space vehicle pointing and the SQUID #3 read-out for a guide star valid period on March 1, 2005.

Table 7: Trapped field in gyroscopes.

Gyro #	Trapped field (μgauss)
1	3.0
2	1.3
3	0.8
4	0.2

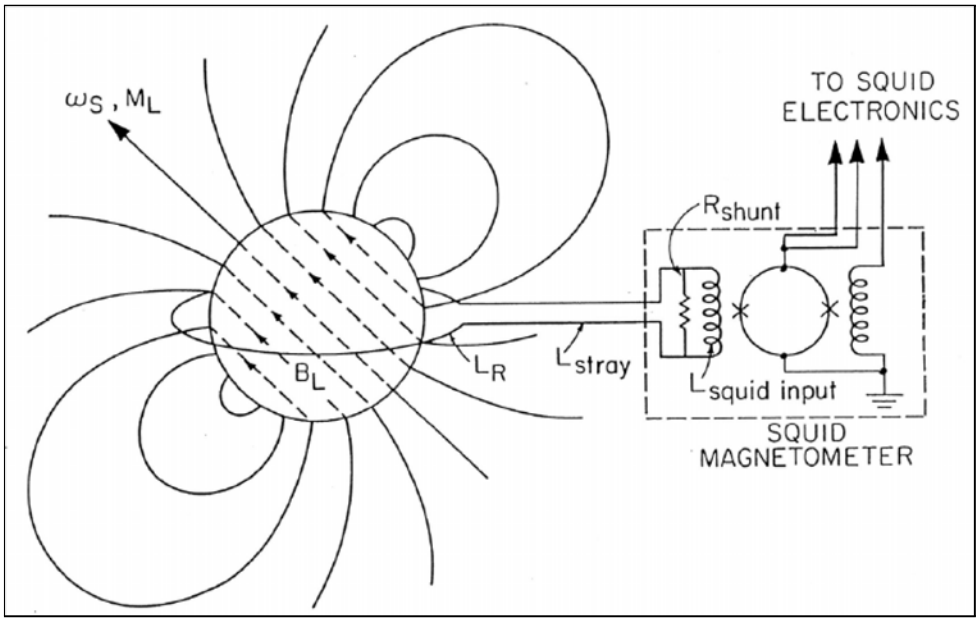

Figure 17: Schematic of GP-B London moment readout.

The proper motion of the guide star HR8703 (IM Pegasus) was determined to better than 0.3 marcs/yr by Very Large Baseline Interferometry using the radio emission of this binary system. IM Peg's identification was confirmed by acquiring neighboring stars in known configuration with respect to it, as well as measuring its well established binary period. Figure 22b and 22c show respectively the stars acquired and the light curve , measured from the ground and in orbit.

The main unexpected experimental observation was the spatial extent of the patch effect on both gyroscope and housing. Patch effects are spatial variations in surface potential caused by non-uniform dipole layers. Ground microscopy and data indicated that the electrostatic patches are of micron size and fraction of volt amplitude. In the low gravity in orbit it was determined

Table 8: SQUID performance in orbit.

SQUID #	Noise at 12.9 mHz ($\mu\Phi_0/\sqrt{Hz}$) SPEC=47.5$\mu\Phi_0/\sqrt{Hz}$	Noise at 12.9 mHz (marcs/$\sqrt{Hz}$) SPEC=190marcs/$\sqrt{Hz}$	SQUID Read-out limit (marcs/yr)
1	28	168	0.198
2	20	157	0.176
3	25	140	0.144
4	24	344	0.348

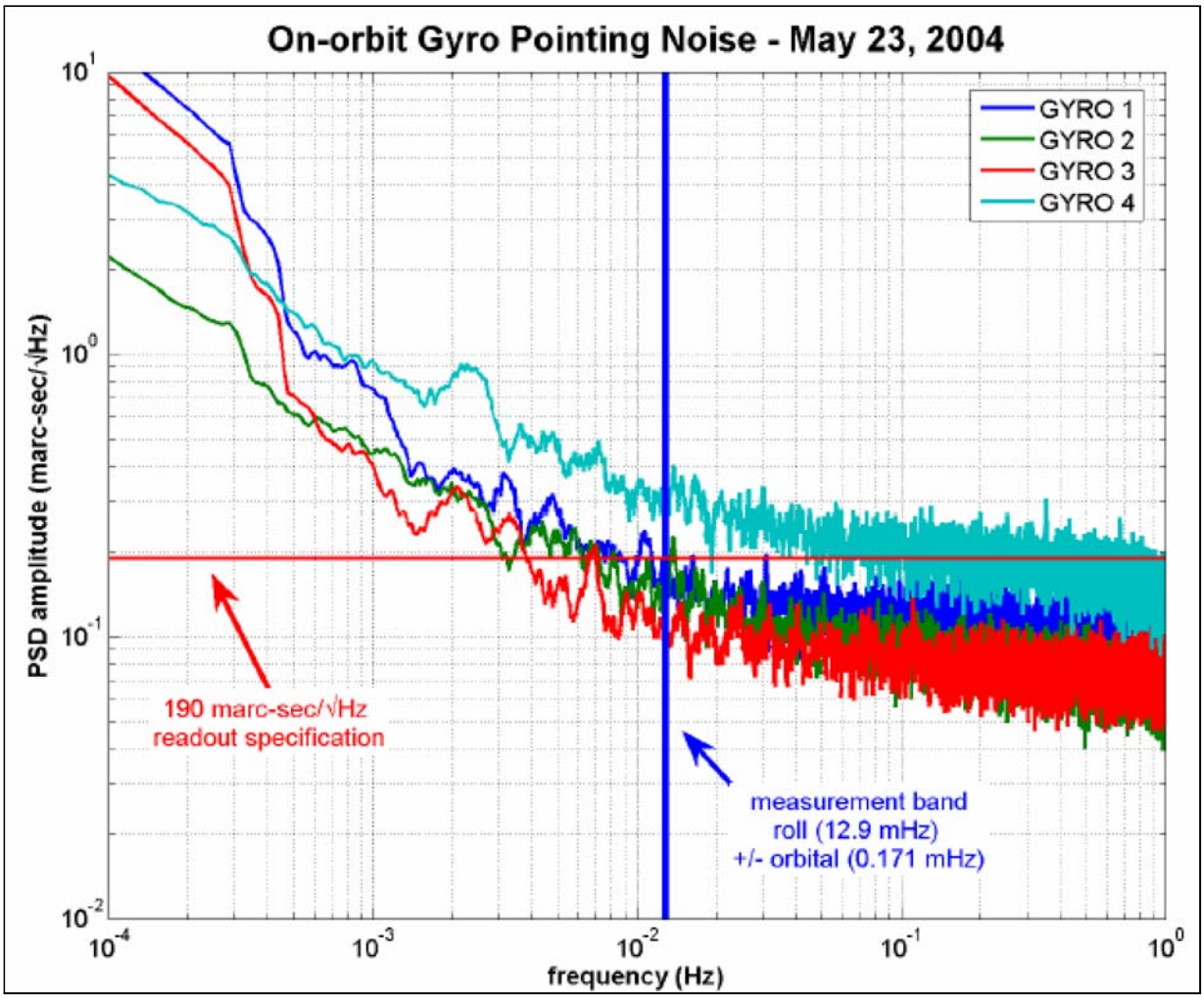

Figure 18: On orbit gyroscope read-out noise.

that size of the patches was up to the order of centimeters. The cause for the patches on the gyroscope was most likely the coherence of the crystalline structure of the thin films over large numbers of single crystals. Misalignment torques, polhode damping and spin-down were the main results of the patch effect.

The experimental observations of excess gyroscope into suspension system coupling were:.

a) The 10^{-9} m/s^{2}space vehicle z (telescope) axis bias modulation at the polhode frequency of the drag free gyroscope; figure 23.

b) Control effort modulation at the 1.3Hz gyroscope spin speed of 2×10^{-7} N, about 30% of total suspension force; figure 24.

c) Position and suspension voltage modulation at the 1.3Hz gyroscope spin speed of 60nm$_{pp}$.

d) Control effort modulation of 10^{-8} N, at polhode frequency, for 80 Hz gyroscope spin speed, about 30% of total suspension force; figure 25.

Rotor geometry cannot account for the magnitude of observed effects. Mass unbalance and surface waviness are of the order of $3\times10^{-3}$of the gap, and would produce effects of the same order of magnitude, about 100 times smaller than the 3×10^{-3} effects observed. Multiple calculations of the interaction of the trapped flux in the rotor with the gyroscope housing have shown that these are orders of magnitude smaller than the measured coupling. However electrostatic patches of 50 mV to 100 mV on both rotor and housing are consistent with all

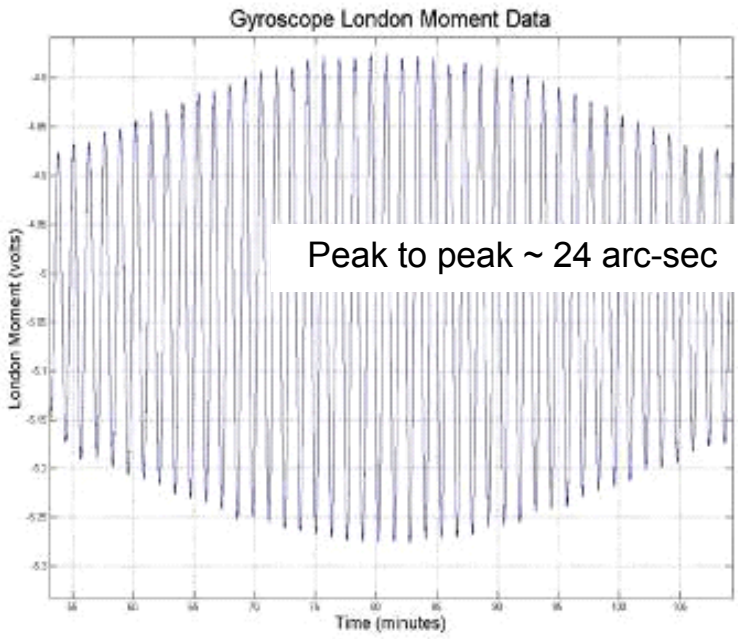

Figure 19: GP-B half orbit SQUID read-out.

observations and predictions.

Misalignment torques cause precession orthogonal to the plane of the misalignment; defined by the gyroscope spin axis and the spacecraft roll axis. Only relativity effects will contribute to angular momentum changes in the misalignment plane. Therefore the accurate measurement of the misalignment angle, including guide star occulted periods makes it possible to separate the precessions due to misalignment torques from those caused by relativity; figure 26a. The misalignment during occultation is measured using the science gyroscopes themselves.

Using the property that misalignment torques are orthogonal to the misalignment angle, the plot of drift rate versus misalignment phase gives a measure of the present consistency between the four gyroscopes, and therefore a measure of the quality of the torque model; figure 27. The schematic in figure 27 shows schematically the method. This analysis approach is called the 'geometric method' by the GP-B team.

Damping of the polhode period changes the trapped flux through the read-out loop and therefore causes variation in the scale factor of the gyroscope. In order to account for this effect in the data analysis high precision knowledge of polhode period and phase is required; figure 26b. These are used as known parameters in the modeling of the gyroscope motion.

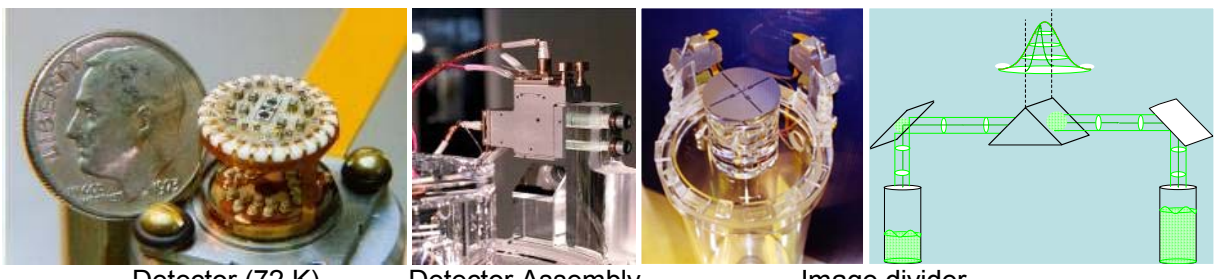

Figure 20: Telescope detector, detector assembly and image divider.

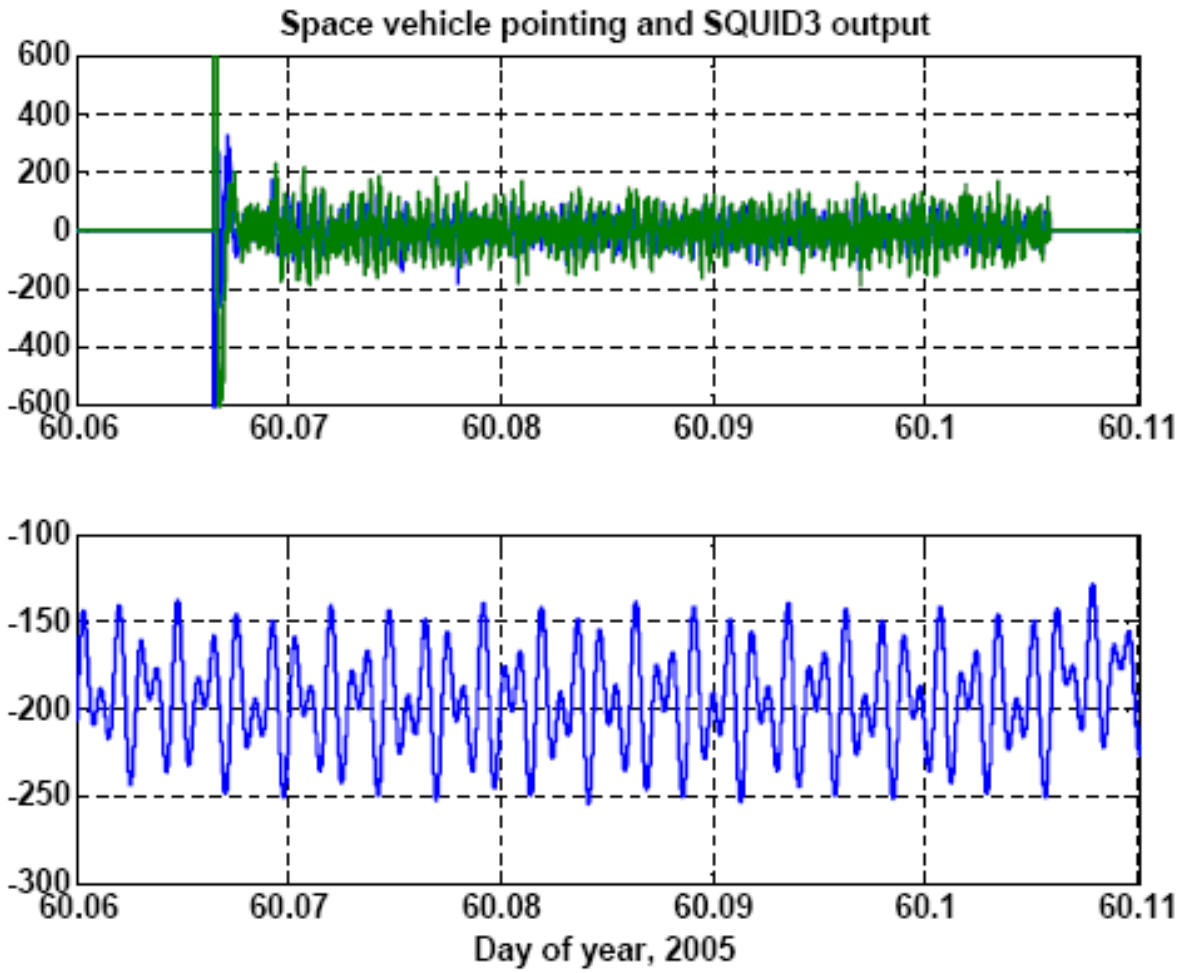

Figure 21: Telescope pointing (top) and SQUID read-out (bottom) for scale factor matching.

The gyroscope spin-down rates (table 4) are equivalent to a gas dissipation pressure of about 10^{-11} torr. However, thermal measurements indicate that the Helium pressure is less than 10^{-14} torr. The excess spin-down is caused by image charges of the gyroscope flowing through the resistors that ground the housing coatings. Patch effect potentials of 40 mV to 80 mV account for the measured spin-down rates. Note that the spin-down rates, independent of their source, meet the GP-B requirement of about 1 μHz/hour. Figure 28 gives the variation of the spin down rate of gyroscope #1 for six months of the mission, with the inset showing a schematic representation of the spin-down dissipation mechanism. Note that the spin-down rate is determined to about 5×10^{-12} Hz/sec.

3 GP-B, LISA, STEP

GP-B, LISA, and STEP are three ultra untypical physics experiments that can meet their precision requirements only by using the quiet environment of space. In particular, the significant technologies overlap of GP-B, LISA,[3] and STEP[4] present us with the opportunity to greatly enhance the probability of success for LISA and STEP by judiciously using the lessons learned from GP-B. The top three of these lessons are the implementation of the simplest most robust design, the use of the most advanced technology available, and the employment of innovative operation methods.

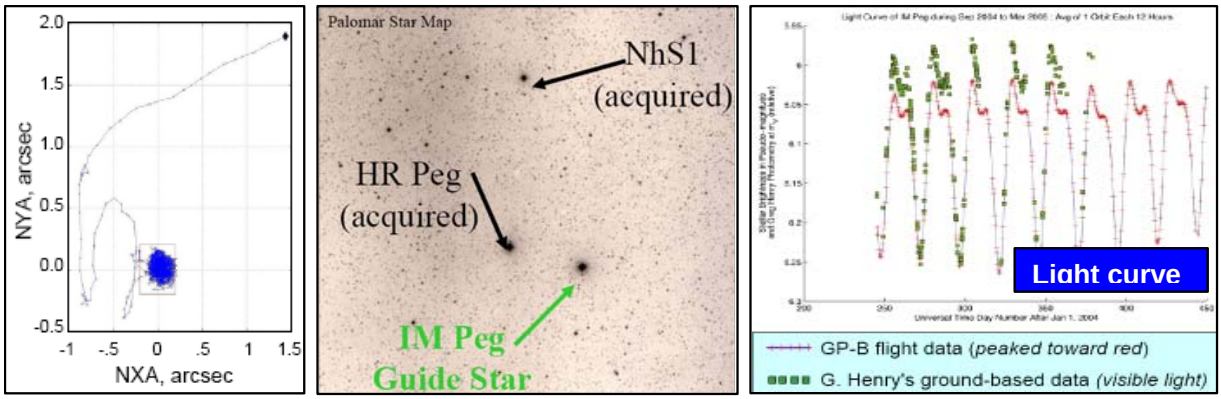

Figure 22: a) GS valid, 54 min.b) Stars acquired near IM Peg. c) Ground and orbit light curves.

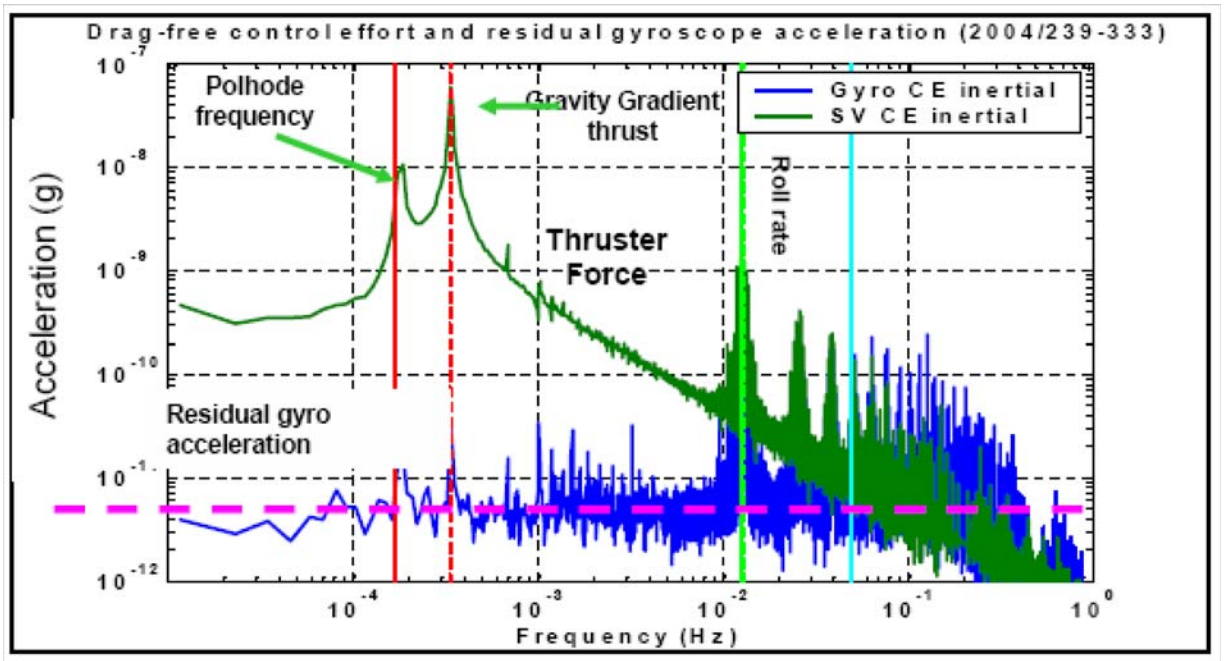

Figure 23: Space vehicle z axis modulation at polhode frequency of drag free sensor.

LISA is a space gravitational wave observatory based on the interferometric measurement of the distances between three spacecraft placed in an equilateral triangle with five million kilometers side. The formation center is twenty degrees behind the Earth on its solar orbit and inclined sixty degrees to the ecliptic, figure 29a. LISA's bandwidth is $3x10^{-5}$ Hz to 1 Hz, complimentary to the ground gravitational wave detectors; figure 29b. LISA takes advantage of the low gravitational environment and the very long baselines available in space. The main GP-B heritage technologies are the gravitational reference sensor (GRS), the high stability optical benches and telescopes, the drag free technology, and the multiple degrees of freedom controls systems. STEP will improve the measurement of the equivalence principle by five orders of magnitude; from 10^{-13} to 10^{-18}. The experiment compares the rate of fall of different materials and relies on the low gravity and the long integration times in a 450 km orbit. The science signal is modulated at orbital frequency; figure 30a. GP-B technologies used for STEP are the cryogenic, magnetic-shielding, drag-free, multiple degrees of freedom controls, and cold gas thrusters systems, the dc SQUID read-out, and the high stability optical bench. Figure 30b

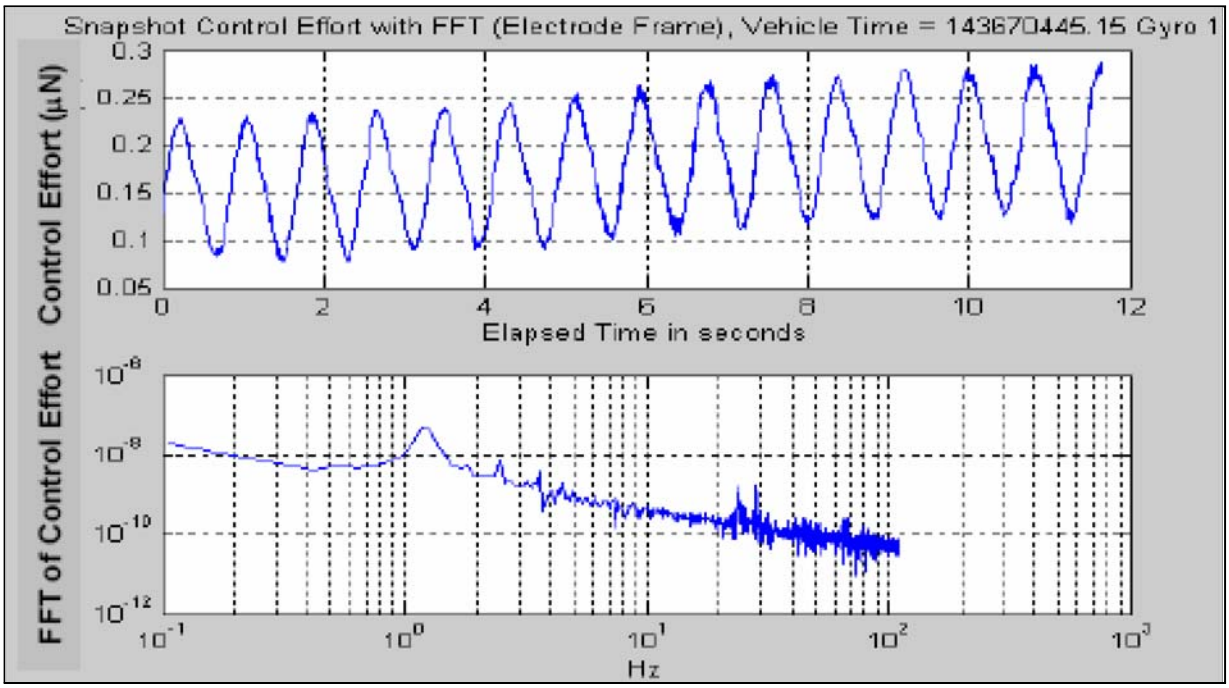

Figure 24: Control effort modulation with gyroscope spinning at 1.3 Hz.

Table 9: Comparaison of significant features of GP-B, STEP and LISA.

	GP-B	STEP	LISA
Measurements/Controls	6	13	16×3
Communications	Ground + TDRSS	Ground + TDRSS	DSN
Drag -free sensors	1	2	6
Formation flying	No (1 satellite)	No (1 satellite)	Yes (3 satellites)
Frequency band	13 mHz	0.18 mHz	$3{\cdot}10^{-5}$Hz to 1 Hz
Drag-free level in band	10^{-12}m/s^2	10^{-11}m/s^2	10^{-11}m/s$^2/\sqrt{Hz}$
Cryogenics	Yes	Yes	No

shows the history of improvements of the equivalence principle measurement.

4 Lessons learned

GP-B, STEP, and LISA have in common sophisticated drag-free attitude and control systems and their payload and vehicles are integrated in a single instrument. Table 9 compares some of their most significant features. Note that while the degrees of control equal the number of independent measurements, each degree of control is activated by more than one actuator, adding further complexity to the experiments.

Lessons learned fall into three main categories; the team, the instrument, and the unexpected. A successful team requires a combination of skills, in this case a close collaboration of physicists and engineers. These instruments are in fact the payload, spacecraft, and control system combined. The approach of designing and building the science payload and the spacecraft separately and then integrating them is unworkable in these experiments were all systems are contributing directly to the experimental error and are expected to perform well beyond the standards of existing space equipment. The lesson is therefore to build a science

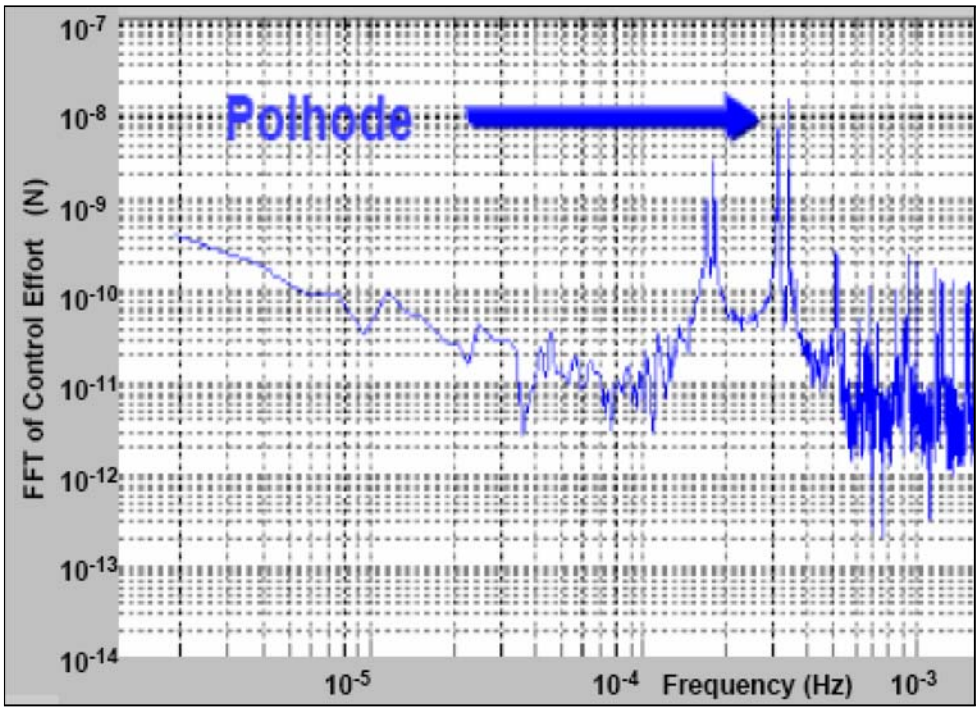

Figure 25: Control effort modulation at polhode frequency with gyroscope spinning at 80 Hz.

and engineering collaboration from the start; engineers with space experience must learn the fundamentals of the science and the scientists need to understand the requirements of work in space. Space experienced personnel are indispensable from the earliest stages of the project in order to include the required knowledge in the design and development; experimenting in space is really very different then working in the laboratory. Students, graduate and undergraduate, are essential to the foundation of the team. Their enthusiasm, hard work, and willingness to undertake 'unsolvable' problems are at the core of the team's performance. And of course they are the future generation of engineers and scientists. Lastly it is imperative to keep the core team for the operations and data analysis stages; it is the team that has build and tested the instrument and its members are the only ones who will be able to operate it successfully in orbit and understand the acquired data. The GP-B core team, including the developers of the instrument, cryogenic systems, and attitude and control system were an integral and critical part of the operations team, and remain at the center of the data analysis team.

Table 9 illustrates not only the similarities but also the difference in technical challenge faced by the three experiments. STEP has the advantage that most technologies involved have been demonstrated by GP-B to the required performance level. LISA has the advantage of not requiring cryogenics. However, in its present configuration, it faces the technical challenges of the many degrees of control for the six drag-free sensors, a restricted communications channel, the need for formation flying, wide frequency band measurement, three orders of magnitude improved drag-free level and complex optical metrology.

The experiment must be instrumented as extensively as possible. Space tests are truly a one-shot opportunity and the experimenter must have maximum opportunity to understand data, anomalies, and calibrations. For the high accuracy tests discussed all system interact to some extent and therefore all need monitoring at five to ten times their maximum operating frequency. Restricting the data telemetry to twice or even a few times the frequency (Nyquist) of the high end of the measurement band is insufficient. Periodical and anomaly-triggered snapshots of the parameters of higher frequency sub-systems are a practical way of understanding their impact

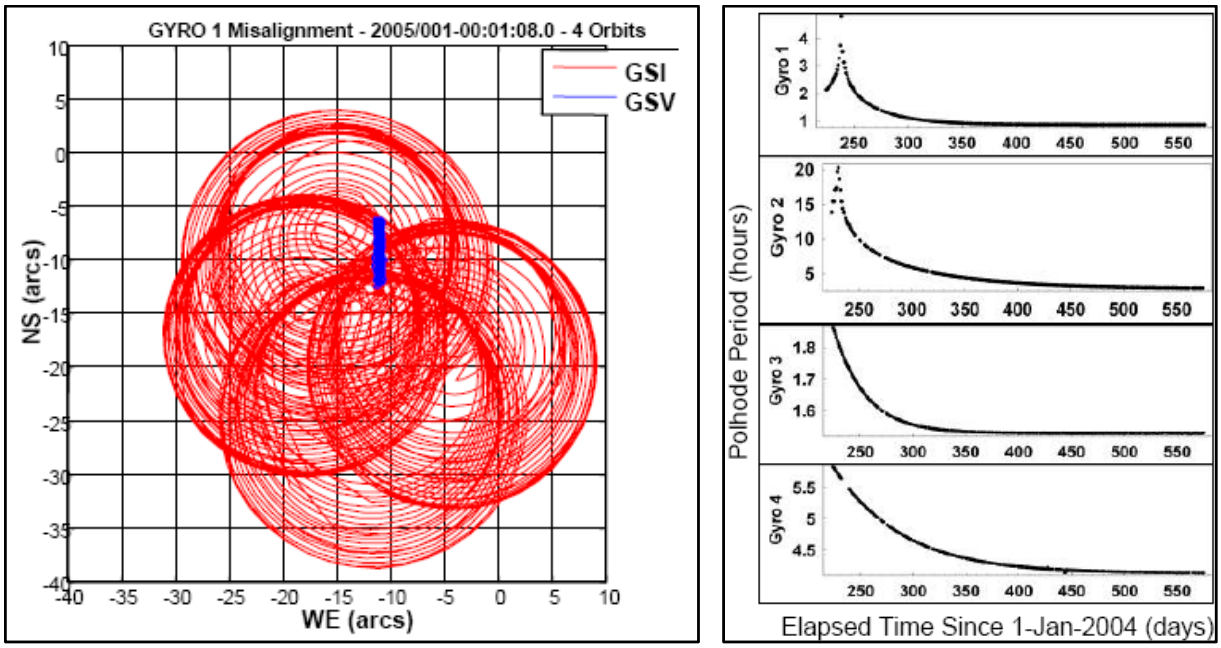

Figure 26: a) Misalignment angle GS valid and invalid. b) Polhode period variation.

on the science data. The GP-B science data was at 13 mHz. Snapshots of the critical electronics, gyroscopes, SQUIDs, and telescope, were collected periodically and for anomalies at sampling frequencies ranging from 220 Hz to 2,200 Hz. These snapshots have proven critical to data analysis and anomaly resolution.

Incremental prototyping is the ideal approach in the development these instruments allowing testing and de-bugging of increasingly complex configurations. The integrated GP-B system went though four incrementally complete system tests. Ground testing should follow the principle "Test it like you fly it". This includes, again in incremental prototyping stages; the instrument, the environment as practical, the flight software, and the telemetry and ground commanding. A high fidelity simulator with hardware in the loop is an essential development, testing, flight operations, and data analysis tool. Development of the simulator starts with a software simulation with hardware prototypes included and ends prior to launch with high fidelity simulations of the instrument using flight hardware software. The simulator includes an identical copy of the mission operations system, making it a virtual science instrument. Following are two, of many, examples of the use of the simulator for anomaly resolution during GP-B operations.

Figure 31a shows the optimization of the in-orbit performance of gyroscope's #2 suspension system. Control loop instability was observed for gyroscope positions more than 2 μm from center; total spacing to suspension electrodes is 32.5 μm. With no risk to the flight instrument, the simulator was used to reproduce the anomaly, find and test a solution, and verify the software and telemetry modifications on the ground before applying them to the experiment in orbit. The simulator accurately reproduced both the anomalous and the optimized performance; the solution was the increase in modulation frequency of the suspension system from 25 Hz to 30 Hz. Note that the anomaly was detected and corrected by the use of gyroscope suspension snapshots, 220 Hz for 12 seconds. The continuous 0.5 Hz data would have clearly been inadequate to the task.

Figure 31b shows the roll frequency component of the attitude control error. The large errors at roll frequency were induced by an anomalous large sensitivity to thermal variations of the platform supporting the navigation instrumentation; the increase in December 2004 coincides

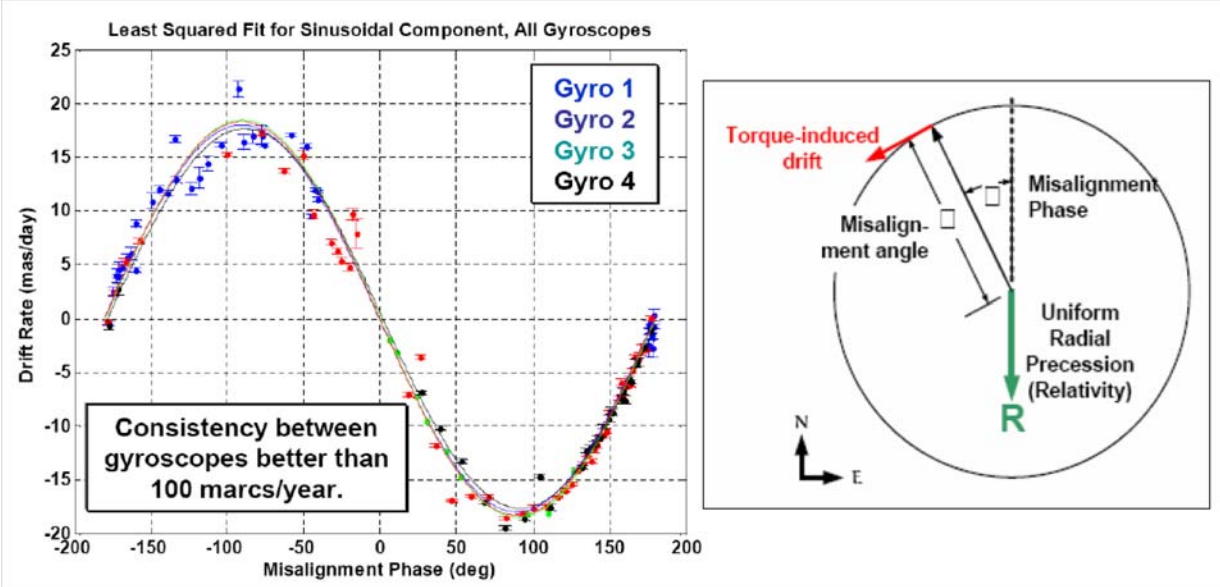

Figure 27: Drift rate versus misalignment phase; the geometric method.

with the GP-B spacecraft moving into full Sun illumination. A notch filter at roll frequency, designed and tested with the simulator, was up-loaded into the flight attitude control system, permanently solving the problem.

The principal technical lessons learned from GP-B including the requirement for a charge control system with wide dynamic range and the importance of the understanding and characterization of surfaces are described in detail in previous sections. Gyroscope charge at levitation was more then ten times larger than accumulated cosmic charging during the entire mission and needed to be removed in hours. The patch effect was the main unexpected disturbance significantly complicating the data analysis.

There are two types of the "unexpected". Real surprises and standard but consistently underestimated difficulties. Rigorous planning can largely mitigate the second category. Required data and commanding rates will be significantly higher than planned for in the early stages of the experiment design; the standard 50% early development contingency should be increase to as much as 100-200%. In particular the experiment set-up stages and anomaly resolution periods will require significantly increased data rates. GP-B data was collected both through the space TDRSS network, ~12 contacts/day, 20-40 minutes/contact, 1-2 Kbits/sec data rate, as well as the ground based network of NASA ground stations, 4 contacts/day, 10-12 minutes/contact, 32 Kbits/sec data rate. The total stored data, including derived monitors and raw and processed data streams is 1.5 Tbytes.

GP-B initial set-up duration was 128 days, versus the planned 40 days plus 20 days contingency, which was expected to be unnecessary. More than 100 anomalies occurred during the mission, including the failure of two thrusters, multiple bit upset events (MBE) at ten times the expected rate, computer reboots, antennas and star sensors degradation. A large percentage of anomalies occurred during initialization, a period that required more than 10,000 commands to the space vehicle for experimental set-up and anomaly resolution. Regarding LISA two significant points of reference are the GP-B 128 days commissioning duration and the five year required by the ground based LIGO to achieve design performance. An aggravating factor is the narrow DSN communication bandwidth as compared to the much faster GP-B telemetry and the non-limiting LIGO instrumental communications capability. LISA requires simulation work at much higher level than any previous mission as well as the development of advanced

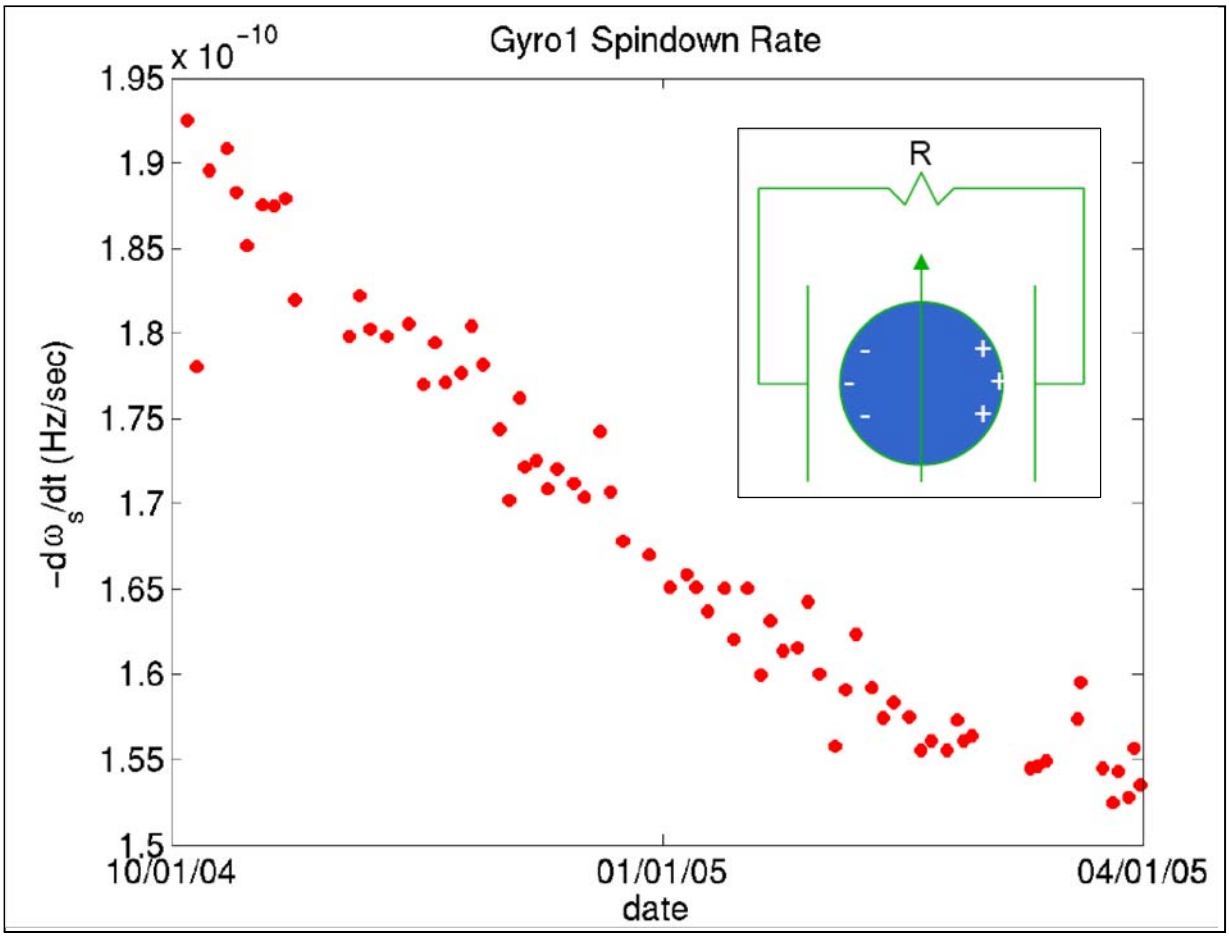

Figure 28: Spin-down rate of gyroscope #1. Insert is a schematic of the spin-down dissipation mechanism.

autonomous software.

Extensive calibrations have proven invaluable for GP-B and have both accurately determined the instrument performance parameters and revealed anomalous behavior. For this class of instruments, designed for minimum sensitivity to disturbance, two methods of calibration are used. Firstly, instrumental performance in planned operating conditions sets an upper limit to their sensitivity. Secondly, operations in a highly degraded controlled environment allow the actual measurement of the effect of the disturbance on the instrument and thus the extrapolation to performance numbers.

Data analysis will always be more complex and time consuming than the most conservative ground estimate. Again contingency scheduling at factors of two to three beyond what is considered "reasonable" on the ground is a very good move. One cannot overemphasize the need for the experience of the core team for data analysis.

A positive aspect of space experimentation is that most systems will work better in this quiet environment. The most complex and apparently risky systems seem to be the best behaved in space; GP-B gyroscope, SQUID's telescope, cryogenics. Experimental plans cannot be based on this fact but in most cases a positive margin of performance is available; and very helpful. The "unknown unknowns", the real surprises, will occur and will by definition be the least expected effects. Preparing for the unexpected is possible through the use of extensive instrumentation and comprehensive data and with the help provided by the experience of the core team.

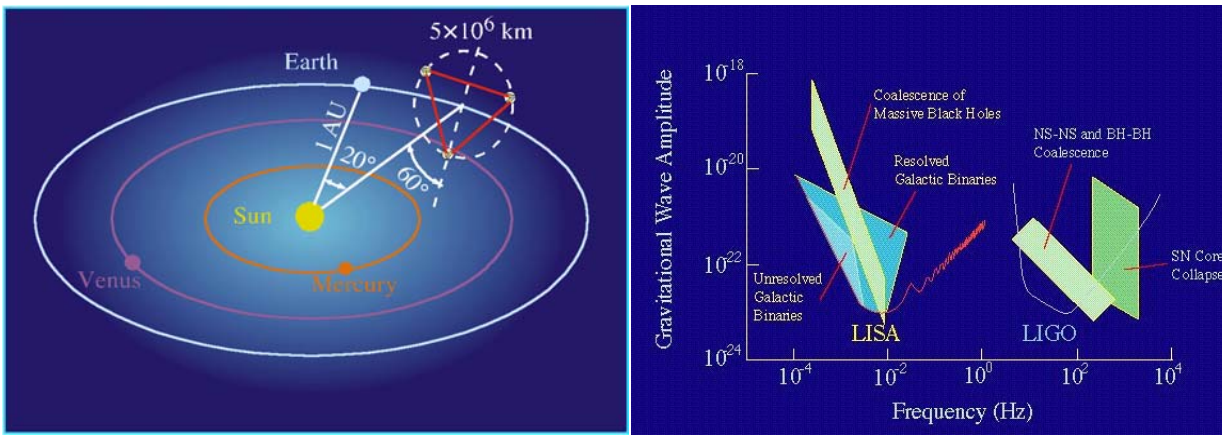

Figure 29: a) LISA concept. b) LISA performance complementary to the LIGO ground detector

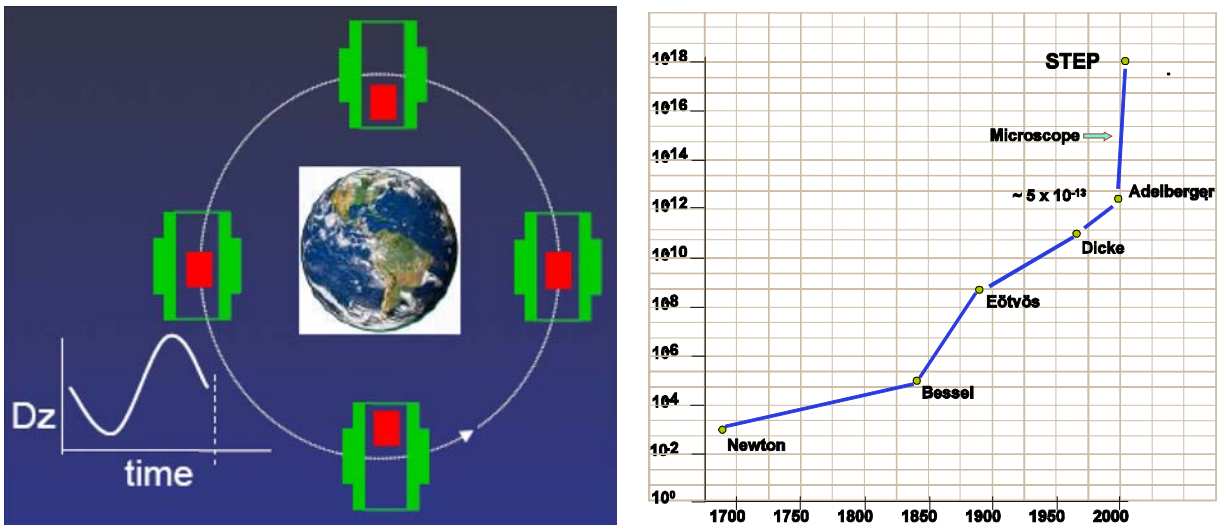

Figure 30: a) STEP concept. b) History of improvements of the equivalence principle measurements

5 Improving Drag-Free: The Modular Gravitational Reference Sensor

The Gravitational Reference Sensor (GRS), by physically shielding a proof mass from stochastic non-gravitational disturbances, provides the basis for following an inertial trajectory. By itself, or when integrated with a complete drag-free control system, the GRS opens new frontiers in Earth imaging and space science; autonomous maintenance and prediction of spacecraft orbits, satellite constellation maintenance without ground tracking, disturbance free inertial trajectories, new observations of the universe through gravity waves, new understanding of the physics of the Universe, precision formation flying for satellite constellation interferometers and imagers, geodesy and surface imaging, integrated precision inertial sensing of translation and rotation, autonomous spacecraft rendezvous, guidance and space-based target tracking.[8]

A Disturbance Reduction System (DRS) is composed of the GRS,the actuating thrusters and the attitude and translation control algorithms. The first drag-free system, called DISCOS, was developed by Stanford University and launched on the U.S. Navy's TRIAD drag-free spacecraft in 1974.[6] Recently, GRS technology found application in space science, lying at the heart of the recently launched NASA Gravity Probe B mission to test Einstein's Theory of Relativity [1]. The GRS will again be crucial to the Laser Interferometer Space Antenna (LISA) [9], part of the

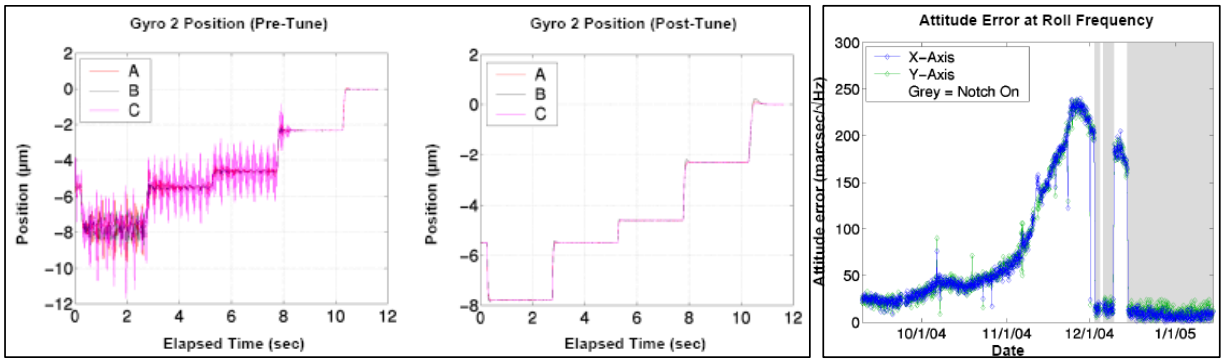

Figure 31: a) Suspension stability pre and post tune. b) Attitude control error at roll frequency; notch filter on in gray areas.

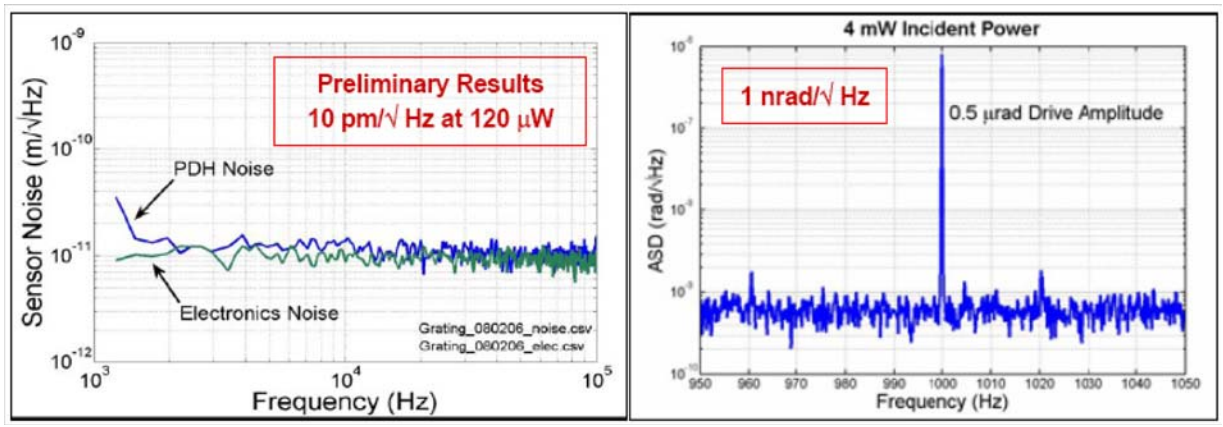

Figure 32: Performance of optical sensors: a) linear, b) angular

NASA SSE Strategic Plan; the LISA GRS will require disturbance reduction improvements of at least four orders of magnitude over current performance.

TRIAD I was launched September 2, 1972 with its Disturbance Compensation System (DISCOS) built by Stanford. Discos had 3 axis translation control and demonstrated an acceleration below 5×10^{-11}m/s^2 averaged over 3 days, corresponding to a residual acceleration of 2.7×10^{-8} m/s$^2/\sqrt{\text{Hz}}$.at 5 μHz.[6] GP-B was launched April 20, 2004 with drag-free control of all degrees of freedom, 3 translations and 3 rotations, and had a residual acceleration of 10^{-11}m/s$^2\sqrt{\text{Hz}}$ at 13 mHz

The three main principles we applied in the design of a modern drag-free sensor are: a) Minimize the forces on the test mass (TM), b) Optimize the TM center of mass determination, and c) Use modern technology; including the optical read-out of the TM position, charge management with UV LEDs, diffraction grating technology, optimized algorithms for TM position determination. . In order to practically eliminate TM forcing we use a non-supported spinning spherical TM. The spin, at about 10 Hz, spectrally shifts the TM measurement noise, (including spin, precession, and polhode) above the science band; 1 Hz for LISA. A gap equal or larger than the TM diameter significantly reduces surface patch effect disturbances. A double sided grating on the sensor housing isolates the GRS from external measurements. The distance from the grating to the TM center of mass is measured directly, making the GRS modular, MGRS, and thus insulating it from other experimental systems.[10] With the TM center of mass measured optically no active electrostatic systems are disturbing the TM. UV LEDs for charge control, gratings for non-transmissive optics advanced interferometry methods, and laser frequency dou-

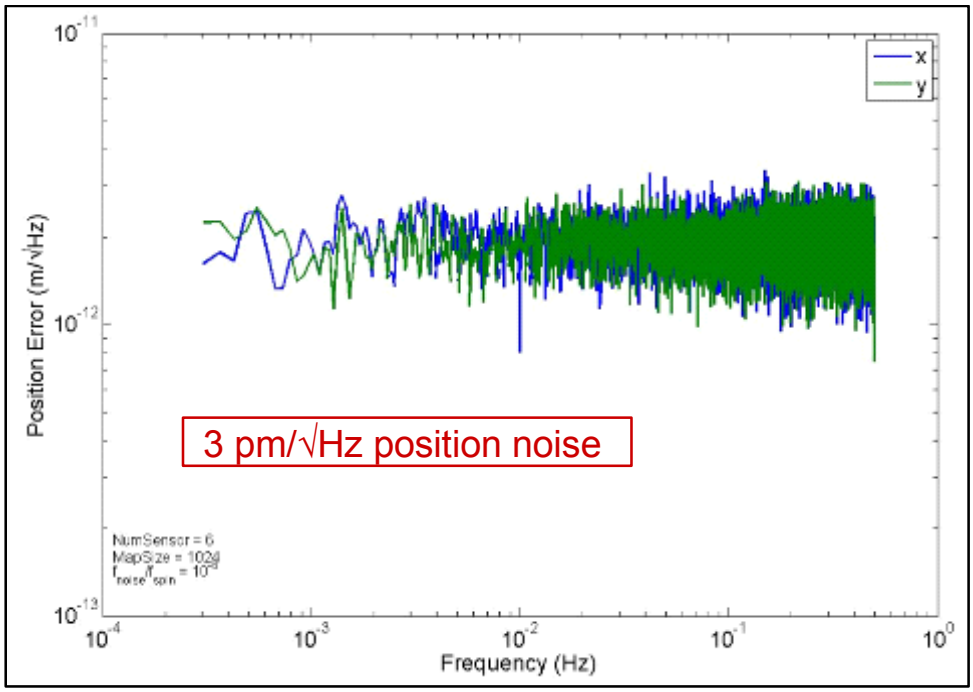

Figure 33: Numerical simulation of optical read-out of 10 Hz spinning sphere.

bling to green are some of the technologies that contribute to solving the challenges of advanced drag-free systems.

Optical sensing offers a high-resolution method of sensing across a large gap while maintaining low disturbances. The sensing element is a low-finesse Fabry-Perot 1.6 cm cavity formed between a Littrow mounted 900 lines/mm diffraction grating and the surface of the proof-mass. The sensor reached 10 pm/$\sqrt{\text{Hz}}$ sensitivity with 120 μW of optical power; figure 32a. Further improvements should achieve 1 pm/$\sqrt{\text{Hz}}$ sensitivity for 20 μW optical power in the LISA science band (3×10^{-5} Hz to 1 Hz).

High precision angular sensing is needed in measuring the TM orientation, telescope steering, and point-ahead-angle control. We have demonstrated the use of grating diffraction orders as angular sensing signal beams, taking advantage of the grating angular magnification. The angular sensitivity achieved is better than 1 nrad/$\sqrt{\text{Hz}}$ with a 6 cm working distance; figure 32b.

A three dimensional numerical simulation of a sphere spinning at 10 Hz has been performed in order to demonstrate the feasibility of measuring the TM center of mass. Six optical sensors, with two sensors in the 60 degrees configuration of the LISA gratings are being used in the model. The position noise and surface roughness of the sphere are 50 nm. The results indicate that the TM center of mass can be measured to 3 pm/$\sqrt{\text{Hz}}$. Further work incorporating additional disturbances is in progress: figure 33.

Since the tip/tilt sensor will require a grating atop the proof mass, we have demonstrated several ways of fabricating gratings on dielectric and gold surfaces: electron-beam lithography, mechanical transfer imprinting, and ion-beam writing. The grating patterns display only small irregularities caused mainly by the step size of the ion beam movement. Measured diffraction efficiencies meet requirements for the MGRS tip/tilt and displacement sensing.

Charge management using photoelectrons has been demonstrated in the GP-B experiment using Hg discharge sources for the generation of the UV .[5] Deep UV LED charge management systems have the advantages of high dynamic range, low disturbance, low power consumption,

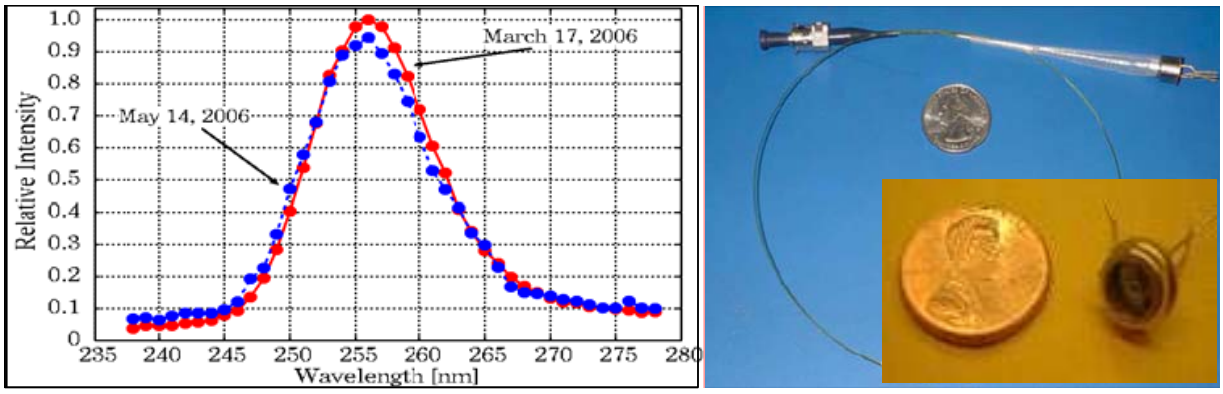

Figure 34: UV LED spectral stability, in TI05 packaging and coupled to optical fiber.

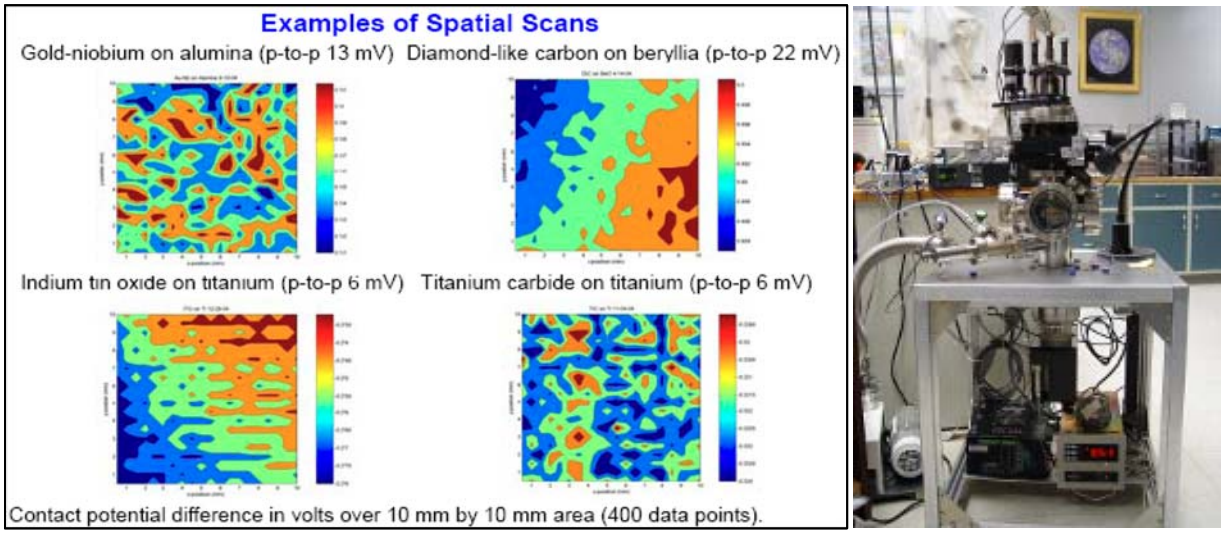

Figure 35: Kelvin probe: a) Spacial scans of coatings, b) Apparatus

and light weight. We have demonstrated AC charge management using a UV LED, and have started the space qualification of these devices A UV LED has operated for more than 8,000 hours under AC charge management working conditions. Additional measurements show power and spectral stability in the UV LED emission over this period of time. Figure 34 shows the UV LED spectral stability over 10 months and photographs of the LED in its TI05 packaging and coupled to an optical fiber.

A major noise source for the MGRS is due to spatial and temporal variations in surface potential (or patch effect) across the surfaces of the test mass and its housing. Such variations will lead to force gradients which will result in a significant acceleration noise term. We have used a Kelvin probe to make spatial and temporal measurements of contact potential differences for a selection of materials (Au/Pt, beryllia, alumina, titanium) and coatings (gold, diamond-like carbon, indium tin oxide, titanium carbide). The data showed evidence of variations in the patch potentials related to pressure and contamination effects. Temporal variation measurements were limited by the current accuracy of the instrument.[11] Figure 35 shows examples of Kelvin probe spacial scans and a photograph of the system.

Conclusions

GP-B, the first controlled experiment in which a General Relativity effect is the main feature of the data, has demonstrated that complex physics experiments do work in space. Preliminary results, in April 2007, set the measurement accuracy at ±97 marcs/yr or about 1.5% of the geodetic effect. Further improvement in accuracy is expected before the end of 2007. LISA and STEP are space physics experiments significantly similar in many features to GP-B. The main lessons that GP-B can convey are: a) a strong core team of scientists and engineers with space experience that works from design to data analysis, b) a flexible, comprehensively monitored and diagnosed instrument, c) significant longer schedule contingency for operations and data analysis, and d) extensive calibrations to ensure results credible to the science community and the experimental team.

Based on the experience and lessons from GP-B, advanced drag-free technology is being developed. The MGRS makes possible the achievement of drag-free performances appropriate for the future generation of space experiments. Among its design features are the complete elimination of electrostatic forcing and sensing, its isolation from other experimental systems, a spherical test mass spinning above the science measurement band, optical linear and angular sensing and gaps larger than the size of the sphere. Technologies that will ensure the performance and reliability of space-based gravitational wave detectors include the MGRS, in-field laser beam pointing, the use of gratings as non-transmissive optics, lasers with frequency doubled to green, and UV LED charge management.

Acknowledgments

This research supported by NASA on contract NAS8-39225

References

1. J. P. Turneaure, et al, *Advances in Space Research* (UK), vol **9**, 29-38 (1989).
2. S. Buchman, et al, *AdvancesinSpaceResearch*; vol.**25**, no.6, 1177-80 (2000).
3. J. E. Faller, et al, *Proceedings of the Colloquium on Kilometric Optical Arrays in Space*, Cargese, Corsica, 23-25 October (1984).
4. P. Worden, A cryogenic test of the equivalence principle *Thesis (Ph.D.)* - Dept. of Physics, Stanford University (1976).
5. S. Buchman, et al, *Rev.Sci.Instrum.* **66**, 120 (1995).
6. D.B. DeBra, *APL Technical Digest*; vol.**12**, no.2, p.14-26 (April-June 1973).
7. J.C. Mester,et. al, *Advances in Space Research*; vol.**25**, no.6, 1185-8 (2000)
8. D. B. DeBra, *Class. Quantum Grav.* **14** (6), 1549 (1997).
9. K. Danzmann and A. Rudiger, *Class. Quantum Grav.* **20** (10), S1 (2003).
10. K. X. Sun, et al., *Class. Quantum Grav.* **22** (10), S287 (2005).
11. N. A. Robertson, et al., *Class. Quantum Grav.* **23** (7), 2665 (2006).